

LS Scienza dei Materiali - a.a. 2006/07

Fisica delle Nanotecnologie – part 5.1

Version 5a, Nov 2006

Francesco Fuso, tel 0502214305, 0502214293 - fuso@df.unipi.it

<http://www.df.unipi.it/~fuso/dida>

Tecniche a scansione di sonda per nanoscopia e nanomanipolazione: STM, AFM e derivati

3/11/2006 – 14.30-16.30 – room T1

10/11/2006 – 14.30-16.30 – room T1

Introduction: need for higher resolution tools I

- Due to diffraction, optical methods fail in providing the required space resolution
- Nanometer or even sub-nanometer resolution can be achieved by using electron microscopy (SEM, TEM)

... **BUT** ...

- Contrast mechanism in electron microscopy are often indirect (they imply many effects)
- Morphology can be quantitatively derived only for the in-plane features (poor info on the relative height)
- Samples must be frequently prepared (made conductive, cut in thin slices,...)
- ***Specific physical quantities (e.g., the local density of states, the magnetic or electrical polarization, the surface optical properties,...) cannot be directly measured***

Ability to measure local (“point”) physical quantities is required to investigate nanotechnology products

Introduction: need for higher resolution tools II

ON THE OTHER HAND

- Optical lithography is unable to provide material control at the desired level
- In a conventional context, electron beam lithography (EBL) can be used with excellent space resolution results

BUT

- Both optical and electron lithographies are thought essentially for top-down approaches
- EBL involves accelerated charges, in a process inherently destructive
- Bottoms-up approaches, based, e.g., on nanoparticles, nanotubes, organics, are hardly compatible with the “aggressive” technology which has been developed for inorganics (silicon technologies)
- ***New, more flexible and more “gentle” techniques must be designed to access the full potential of nanotechnologies, at least in the laboratory environment (i.e., not necessarily suited for the industry)***

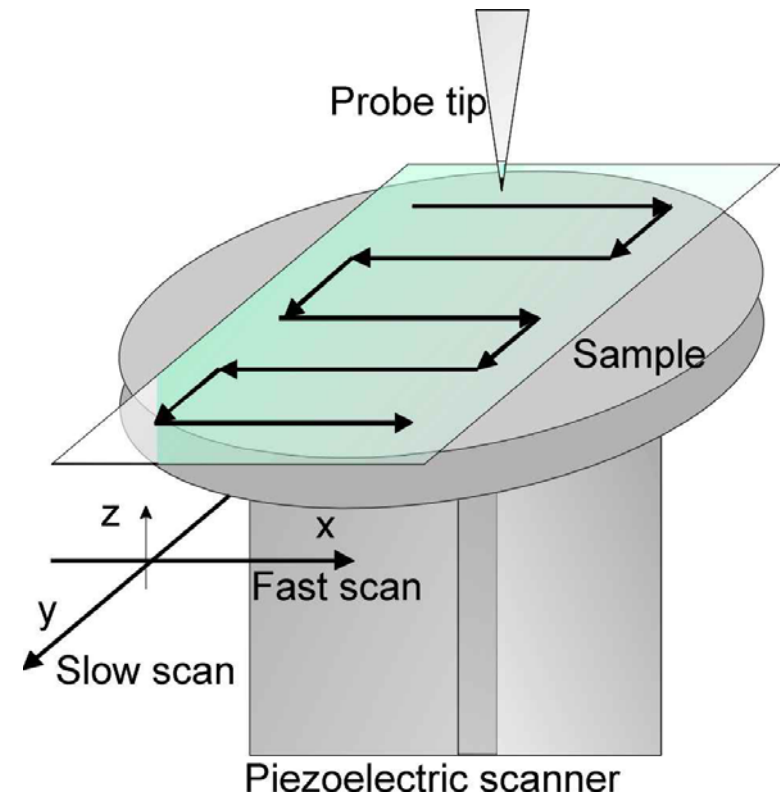
Ability to manipulate the matter at the nanometer level is required to produce new nanotechnology

Basics of Scanning Probe Microscopy (SPM)

Scanning: piezoelectric translator
Probe: tip probing local properties
Microscopy: sub-micrometer resolution
(+ system to control tip/sample distance
+ electronics for instrument operation)

Developed starting since '80s thanks to:

- ✓ Piezo translators with sub-nm resolution;
- ✓ sub-nm probes



Various physical quantities can be measured point-by-point during the scan and an image (i.e., a map of the quantity) can be built up

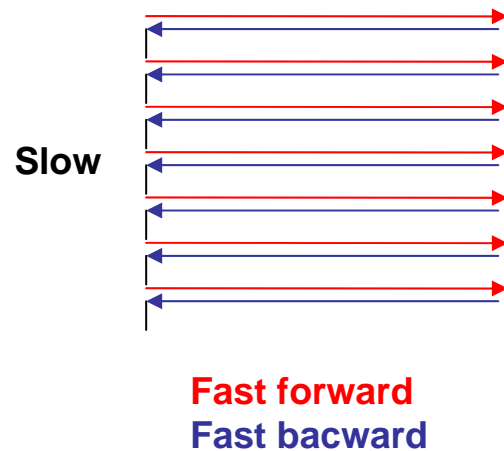
A few examples of SPMs

Technique	Probed quantity	Resolution
SFM	STM	Electron tunneling
	AFM	Mechanical force
	SFFM	Friction force
	MFM	Local magnetization
	EFM	Local polarization
	SNOM	Optical properties
	Ap-SNOM	Optical properties
...



Depending on the probe and on its interaction with the surface, a variety of physical effects can be investigated

A few preliminary considerations on scans



Normally, a **raster scan** is applied:

- Scan addresses an array of discrete, equispaced “pixels” (e.g., 64x64, 128x128, 256x256,...);
- Scan speed is different for one and the other directions (**fast and slow** scans, respectively);
- **Forward** (trace) and **backward** (retrace) scans along the “fast axis” are typically acquired;
- Forward/backward **comparison** is routinely used to assess the scan quality (unless it is used to derive some physical quantity, as in LFM)

The acquisition speeds depends on:

- Time response of the scanner (typically a few ms for nm-sized displacements);
- The signal-to-noise of the quantity to be probed and acquired (through μs to s depending on the nature of the measurement)

**Rule of thumb: fast acquisition are more suited to higher resolution
(in order to prevent thermal and mechanical drifts)**

A few details: piezoelectric scanner

The piezoelectric coefficient d is negative representing contraction perpendicular to the field; and positive for strain measured along the 3-direction (along which the thickness t is measured) representing expansion parallel to the electric field direction:

$$\Delta t = d_{33} V .$$

(4.4)

Although there are many ceramic compositions used today, most can be placed into two general categories: hard and soft PZT materials. Typical d coefficients for hard PZT materials are

$$d_{33} = 250 \cdot 10^{-12} \text{ m/V} , \quad d_{31} = -110 \cdot 10^{-12} \text{ m/V} ;$$

and for soft PZT materials

$$d_{33} = 600 \cdot 10^{-12} \text{ m/V} , \quad d_{31} = -270 \cdot 10^{-12} \text{ m/V} .$$

For PZT-5H

$$d_{33} = 593 \cdot 10^{-12} \text{ m/V} , \quad d_{31} = -273 \cdot 10^{-12} \text{ m/V} .$$

Displacement as small as $\sim 0.1\text{-}0.5$ nm/V (along Z) are possible

Typical "scanner sensitivity":

$\sim 1\text{-}10$ nm/V (along Z)

$\sim 1\text{-}100$ nm/V (along XY)

Typical driving voltages up to ± 250 V

Typical min driving step size (16 bit)

~ 10 mV

Typ: hollow tubes made of PZT-based ceramics with a multi-electrode configuration aimed at controlling the displacement along different directions.

Main issues:

- Linearity (possibly closed loop);
- Hysteresis;
- Distorted motion (*artifacts*).

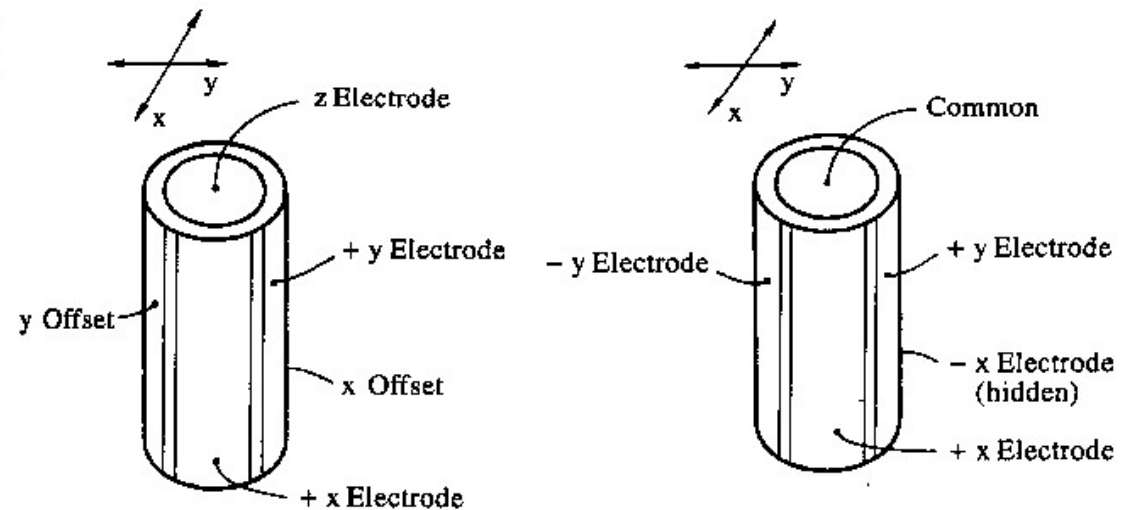


Fig. 4.5. Illustrating the voltages applied to the electrodes of the single-tube scanner

Scanner-related artifacts I

Artifacts mean the presence of spurious information in an SPM image
The easiest way to approach the artifact problem is in AFM (we'll see soon how it works!)

2.0 Scanner Artifacts

Scanners that move the probe in an atomic force microscope in the X, Y and Z directions are typically made from piezoelectric ceramics. As electromechanical transducers, piezoelectric ceramics are capable of moving a probe very small distances. However, when a linear voltage ramp is applied to piezoelectric ceramics, the ceramics move in a nonlinear motion. Further, the piezoelectric ceramics exhibit hysteresis effects caused by self-heating. Artifacts can also be introduced into images because of the geometry of the scanner. The positioning of the scanner relative to the sample can also create artifacts.

2.2. X-Y Calibration/Linearity

All atomic force microscopes must be calibrated in the X-Y axis so that the images presented on the computer screen are accurate. Also the motion of the scanners must be linear so that the distances measured from the images are accurate. With no correction, the features on an image will typically appear smaller on one side of the image than on the other.

2.6. Scanner Drift

Drift in AFM images can occur because of thermal drift in the piezoelectric scanner and because an AFM can be susceptible to external temperature changes. The most common type of drift occurs at the beginning of a scan of a zoomed-in region of an image. This artifact causes the initial part of a scan range to appear distorted. Drift artifacts are most easily observed when imaging test patterns. Drift will cause lines that should appear straight to have curvature.

Figure 16

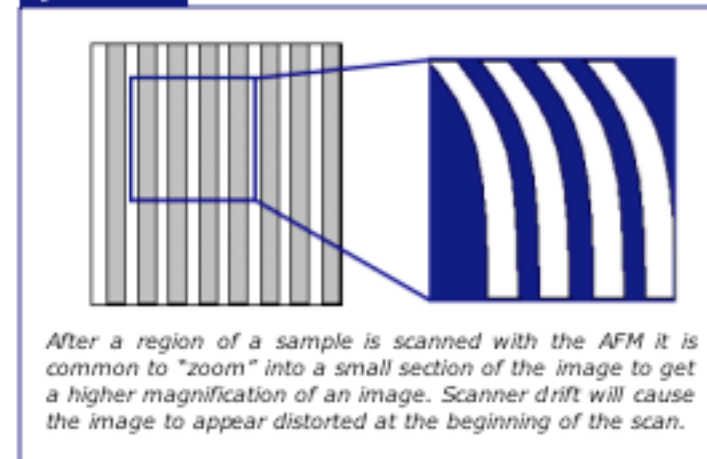
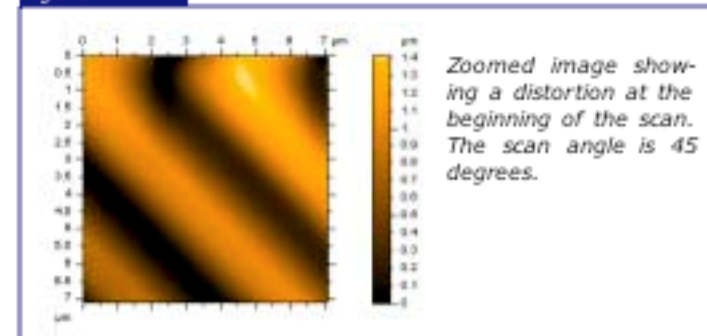


Figure 17



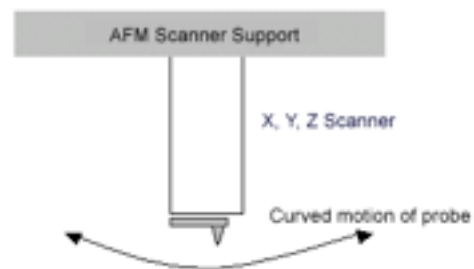
Scanner-related artifacts II

2.4. Background Bow/Tilt

The piezoelectric scanners that move the probe in an atomic force microscope typically move the probe in a curved motion over the surface. The curved motion results in a "Bow" in the AFM image. Also, a large planar background or "Tilt" can be observed if the probe/sample angle is not perpendicular.

Often the images measured by the AFM include a background "Bow" and a background "Tilt" that are larger than the features of interest. In such cases the background must be subtracted from the image. This is often called "leveling" or "flattening" the image. After "leveling" the desired features are typically directly seen in the image.

Figure 12



An AFM piezoelectric scanner is often supported at the top by a mechanical assembly. Thus the motion of the probe is nonlinear in the Z axis as it is scanned across a surface. The motion can be spherical or even parabolic depending on the type of piezoelectric scanner.

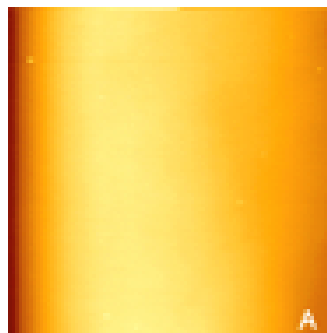


Figure 13A-B: Image (A) is an 85 X 85 micron image of a flat piece of silicon. The bow introduced into the image is seen at the edges. (B) A line profile across this image shows the magnitude of the bow.

(Image) post-processing can help
(but can also introduce new artifacts, as well...)

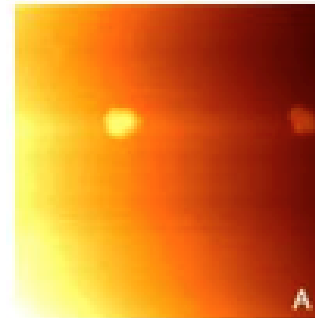
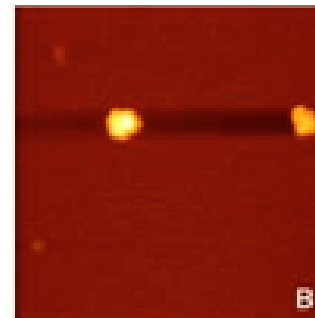
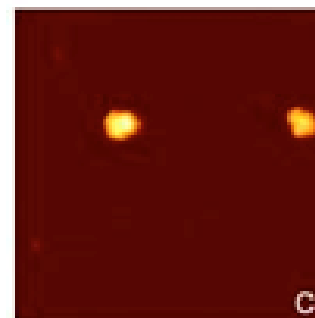


Figure 21A-C: AFM images a 1.6 X 1.6 micron image of nanospheres on a surface.

(A) The original image measured by the AFM before any image processing. Tilt is easily recognized in the image as the right side of the image appears darker than the left side of the image.



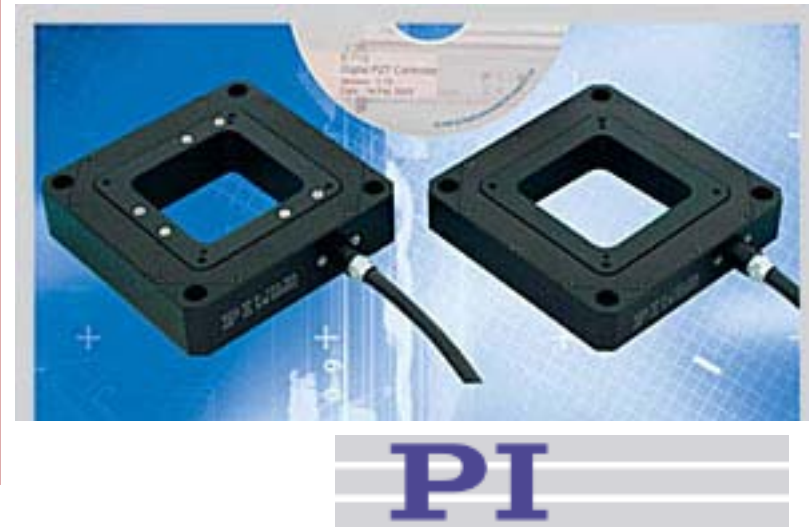
(B) The AFM image shown in "A" after a line-by-line leveling of the image with a first order background correction. The dark band in the image is caused by the image processing and is not a real structure.



(C) Particles are excluded from the background subtraction process to derive this image.

Closed-loop scanners

- ✓ Problems associated with the scanner geometry can be solved by using different scanner configurations (e.g., non cylindrical)
- ✓ Problems associated with non-linearity, hysteresis, drifts, can be solved by using closed-loop scanners (displacement is independently measured, e.g., by capacitive or interferometric or resistive means, and a loop is applied)



Excellent performances presently achievable

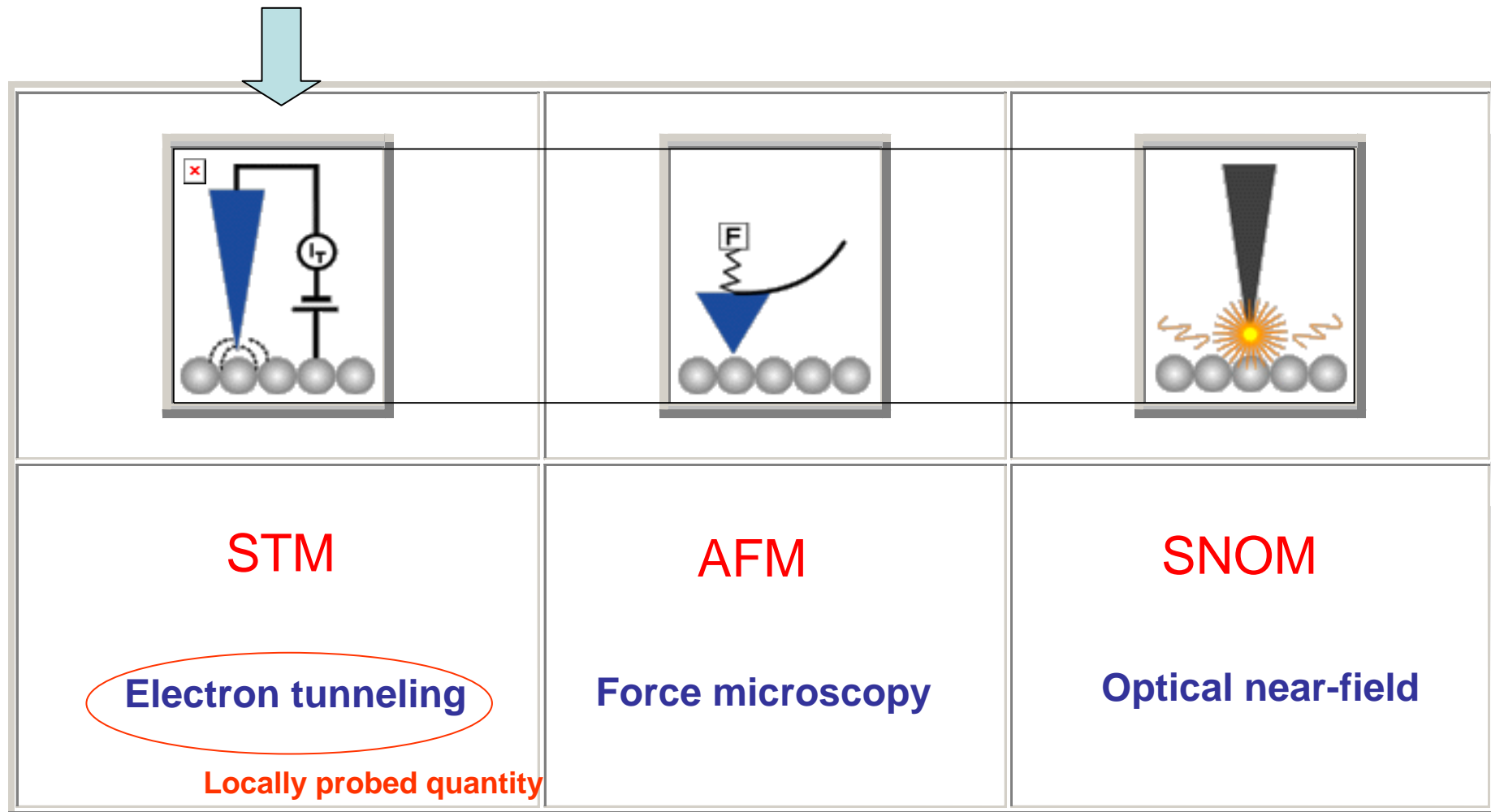
Nanometer Accuracy in 1 Millisecond with 50-Picometer Resolution
PicoCube® systems provide resolution of 50 picometers and below. The ultra-fast XY/XYZ piezo drives offer resonant frequencies of 9.8 kHz in Z and >3 kHz in X and Y! The high resonant frequency and high-bandwidth capacitive feedback allow step and settle to 1% accuracy in as little as one millisecond.



Outlook

1. The mother of all SPMs: Scanning Tunneling Microscopy (STM): mechanisms and instruments to investigate local electronic properties
2. SPM based on probing mechanical forces:
 - A. Atomic Force Microscopy (AFM): contact and non contact modes
 - B. Variants (lateral, electrostatic, magnetic forces,...)
3. Sub-diffraction properties of electromagnetic waves:
 - A. Scanning Near Field Optical Microscopy (SNOM);
 - B. Polarization-Modulation SNOM
4. “Lithographies” (better denoted as “nanomanipulations”) associated with:
 - A. STM;
 - B. AFM;
 - C. SNOM

1. Scanning Tunneling Microscopy (STM)



Historically, STM is the first working realization of SPM, and probably the simplest

STM tip (probe) preparation

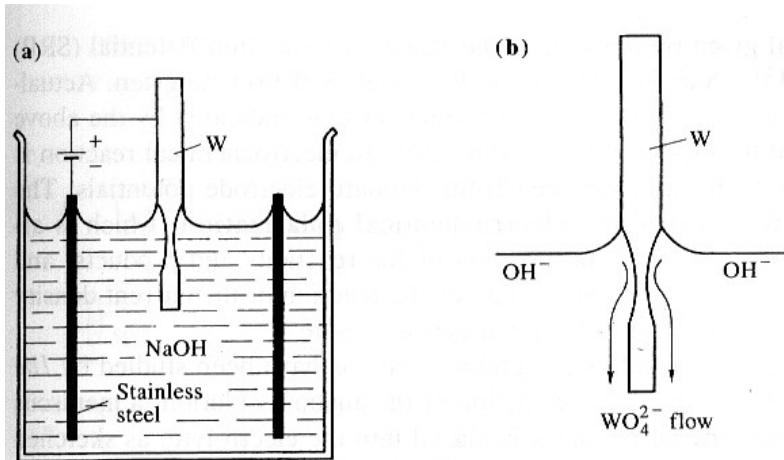
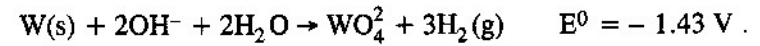
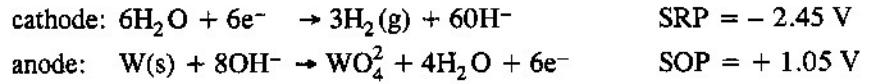
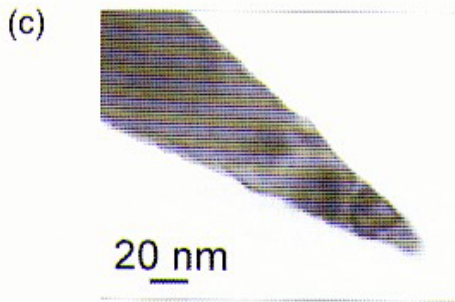
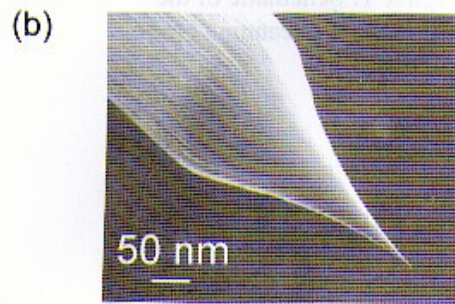


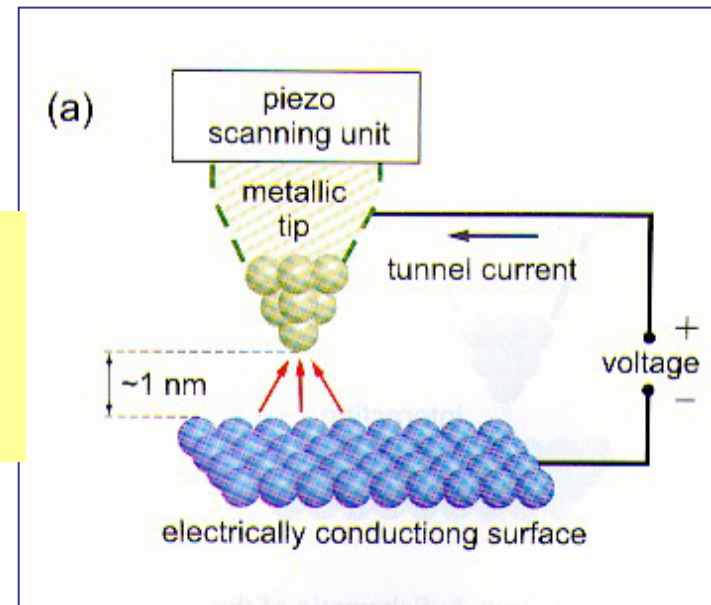
Fig. 4.12. (a) Schematic diagram of the electrochemical cell showing the tungsten wire (anode) being etched in NaOH. The cathode consists of a stainless-steel cylinder which surrounds the anode. (b) Sketch of the etching mechanism showing the "flow" of the tungstate anion down the sides of wire in solution [4.13]



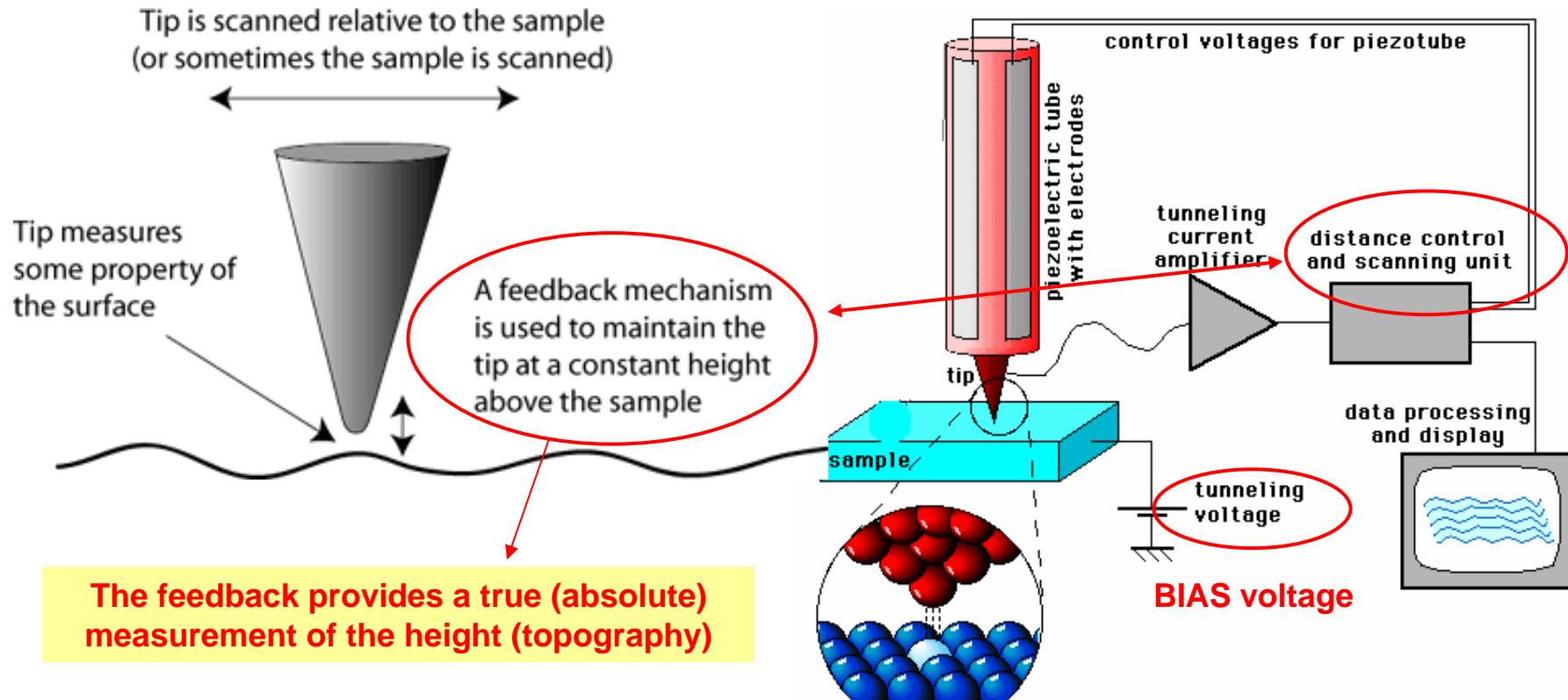
Electrochemical etching of W or Pt/Ir typically used



Very sharp tips can be obtained (ideally, terminated by a "single" atom)



Basics of Scanning Tunneling Microscopy



STM:

- ✓ Probe is a conductive tip
- ✓ Sample (surface) is mostly conductive or semiconductive
- ✓ A bias voltage is applied between sample and tip
- ✓ Tip is kept at small distance from the surface (typ < 1 nm)
- ✓ Tunneling current (typ in the pA range) is measured

Reminders of tunnel effect I

Da Eisberg Resnick, Quantum Physics
Wiley (1985)

For the barrier potential of (6-45), we know from the qualitative arguments of the last chapter that acceptable solutions to the time-independent Schrodinger equation should exist for all values of the total energy $E \geq 0$. We also know that the equation breaks up into three separate equations for the three regions: $x < 0$ (left of the barrier), $0 < x < a$ (within the barrier), and $x > a$ (right of the barrier). In the regions to the left and to the right of the barrier the equations are those for a free particle of total energy E . Their general solutions are

$$\begin{aligned} \psi(x) &= Ae^{ik_1x} + Be^{-ik_1x} & x < 0 \\ \psi(x) &= Ce^{ik_1x} + De^{-ik_1x} & x > a \end{aligned} \quad (6-46)$$

where

$$k_1 = \frac{\sqrt{2mE}}{\hbar}$$

In the region within the barrier, the form of the equation, and of its general solution, depends on whether $E < V_0$ or $E > V_0$. Both of these cases have been treated in the previous sections. In the first case, $E < V_0$, the general solution is

$$\psi(x) = Fe^{-k_{II}x} + Ge^{k_{II}x} \quad 0 < x < a \quad (6-47)$$

where

$$k_{II} = \frac{\sqrt{2m(V_0 - E)}}{\hbar} \quad E < V_0$$

In the second case, $E > V_0$, it is

$$\psi(x) = Fe^{ik_{III}x} + Ge^{-ik_{III}x} \quad 0 < x < a \quad (6-48)$$

where

$$k_{III} = \frac{\sqrt{2m(E - V_0)}}{\hbar} \quad E > V_0$$

Note that (6-47) involves real exponentials, whereas (6-46) and (6-48) involve complex exponentials.

Since we are considering the case of a particle incident on the barrier from the left, in the region to the right of the barrier there can be only a transmitted wave as there is nothing in that region to produce a reflection. Thus we can set

$$D = 0$$

In the present situation, however, we cannot set $G = 0$ in (6-47) since the value of x is limited in the barrier region, $0 < x < a$, so $\psi(x)$ for $E < V_0$ cannot become infinitely large even if the increasing exponential is present. Nor can we set $G = 0$ in (6-48) since $\psi(x)$ for $E > V_0$ will have a reflected component in the barrier region that arises from the potential discontinuity at $x = a$.

We consider first the case in which the energy of the particle is less than the height of the barrier, i.e., the case:

$$E < V_0$$

In matching $\psi(x)$ and $d\psi(x)/dx$ at the points $x = 0$ and $x = a$, four equations in the arbitrary constants A, B, C, F , and G will be obtained. These equations can be used to evaluate B, C, F , and G in terms of A . The value of A determines the amplitude of the eigenfunction, and it can be left arbitrary. The form of the probability density corresponding to the eigenfunction obtained is indicated in Figure 6-14 for a typical situation. In the region $x > a$ the wave function is a pure traveling wave and so the probability density is constant, as for $x > 0$ in Figure 6-10. In the region $x < 0$ the wave function is principally a standing wave but has a small traveling wave component because the reflected traveling wave has an amplitude less than that of the

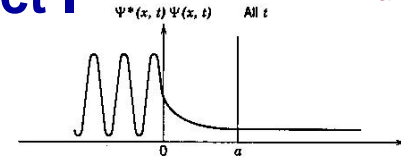


Figure 6-14 The probability density function $\Psi^*\Psi$ for a typical barrier penetration situation.

incident wave. So the probability density in that region oscillates but has minimum values somewhat greater than zero, as for $x < 0$ in Figure 6-10. In the region $0 < x < a$ the wave function has components of both types, but it is principally a standing wave of exponentially decreasing amplitude, and this behavior can be seen in the behavior of the probability density in the region.

The most interesting result of the calculation is the ratio T , of the probability flux transmitted through the barrier into the region $x > a$, to the probability flux incident upon the barrier. This transmission coefficient is found to be

$$T = \frac{v_1 C^* C}{v_1 A^* A} = \left[1 + \frac{(e^{k_{II}a} - e^{-k_{II}a})^2}{16 \frac{E}{V_0} \left(1 - \frac{E}{V_0}\right)} \right]^{-1} = \left[1 + \frac{\sinh^2 k_{II}a}{4 \frac{E}{V_0} \left(1 - \frac{E}{V_0}\right)} \right]^{-1} \quad (6-49)$$

where

$$k_{II}a = \sqrt{\frac{2mV_0a^2}{\hbar^2} \left(1 - \frac{E}{V_0}\right)} \quad E < V_0$$

If the exponents are very large, this formula reduces to

$$T \approx 16 \frac{E}{V_0} \left(1 - \frac{E}{V_0}\right) e^{-2k_{II}a} \quad k_{II}a \gg 1 \quad (6-50)$$

as can be verified with ease. When (6-50) is a good approximation, T is extremely small.

These equations make a prediction which is, from the point of view of classical mechanics, very remarkable. They say that a particle of mass m and total energy E , incident on a potential barrier of height $V_0 > E$ and finite thickness a , actually has a certain probability T of penetrating the barrier and appearing on the other side. This phenomenon is called barrier penetration, and the particle is said to tunnel through the barrier. Of course, T is vanishingly small in the classical limit because in that limit the quantity $2mV_0a^2/\hbar^2$, which is a measure of the opacity of the barrier, is extremely large.

We shall discuss barrier penetration in detail shortly, but let us first finish describing the calculations by considering the case in which the energy of the particle is greater than the height of the barrier, i.e., the case:

$$E > V_0$$

In this case the eigenfunction is oscillatory in all three regions, but of longer wavelength in the barrier region, $0 < x < a$. Evaluation of the constants B, C, F , and G by application of the continuity conditions at $x = 0$ and $x = a$, leads to the following formula for the transmission coefficient

$$T = \frac{v_1 C^* C}{v_1 A^* A} = \left[1 - \frac{(e^{ik_{III}a} - e^{-ik_{III}a})^2}{16 \frac{E}{V_0} \left(\frac{E}{V_0} - 1\right)} \right]^{-1} = \left[1 + \frac{\sin^2 k_{III}a}{4 \frac{E}{V_0} \left(\frac{E}{V_0} - 1\right)} \right]^{-1} \quad (6-51)$$

where

$$k_{III}a = \sqrt{\frac{2mV_0a^2}{\hbar^2} \left(\frac{E}{V_0} - 1\right)} \quad E > V_0$$

Depends on E/V_0 and a

Reminders of tunnel effect II

Da Eisberg Resnick, Quantum Physics Wiley (1985)

Table 6-2. A Summary of the Systems Studied in Chapter 6

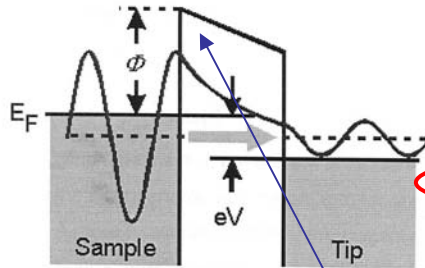
Name of System	Physical Example	Potential and Total Energies	Probability Density	Significant Feature
Zero potential	Proton in beam from cyclotron			Results used for other systems
Step potential (energy below top)	Conduction electron near surface of metal			Penetration of excluded region
Step potential (energy above top)	Neutron trying to escape nucleus			Partial reflection at potential discontinuity
Barrier potential (energy below top)	alpha particle trying to escape Coloumb barrier			Tunneling
Barrier potential (energy above top)	Electron scattering from negatively ionized atom			No reflection at certain energies
Finite square well potential	Neutron bound in nucleus			Energy quantization
Infinite square well potential	Molecule strictly confined to box			Approximation to finite square well
Simple harmonic oscillator potential	Atom of vibrating diatomic molecule			Zero-point energy



Single barrier tunneling

(Single barrier) tunneling of electrons through tip and surface (or vice versa, depending on bias polarity) is the key point of STM

More on tunneling current



2.1. Electron Tunneling

In classical physics an electron cannot penetrate into or across a potential barrier if its energy E is smaller than the potential Φ within the barrier. A quantum mechanical treatment predicts an exponential decaying solution for the electron wave function in the barrier. For a rectangular barrier we get

$$\Psi(d) = \Psi(0)e^{-\kappa d} \quad \text{where } \kappa = \frac{\sqrt{2m(\Phi - E)}}{\hbar} \quad \text{Extinction length}$$

The probability of finding an electron behind the barrier of the width d is

$$W(d) = |\Psi(d)|^2 = |\Psi(0)|^2 e^{-2\kappa d} \quad \text{Exponential decrease}$$

In scanning tunneling microscopy a small bias voltage V is applied so that due to the electric field the tunneling of electrons results in a tunneling current I . The height of the barrier can roughly be approximated by the average workfunction of sample and tip.

$$\Phi = 1/2(\Phi_{\text{sample}} + \Phi_{\text{tip}})$$

If the voltage is much smaller than the workfunction $eV \ll \Phi$, the inverse decay length for all tunneling electrons can be simplified to

$$\kappa \approx \frac{\sqrt{2m\Phi}}{\hbar} \quad \text{Typ } \kappa \sim 10^{10} \text{ m}^{-1}$$

The current is proportional to the probability of electrons to tunnel through the barrier:

$$I \propto \sum_{E_n=E_F-eV}^{E_F} |\Psi_n(0)|^2 e^{-2\kappa d}$$

By using the definition of the local density of states for $\epsilon \rightarrow 0$

$$\rho(z, E) \equiv \frac{1}{\epsilon} \sum_{E_n=E-\epsilon}^E |\Psi_n(z)|^2 \quad \leftarrow \text{Local density of states (a definition)}$$

the current can be expressed by

$$I \propto V \rho_{sa}(0, E_F) e^{-2\kappa d} \quad (*)$$

$$\approx V \rho_{sa}(0, E_F) e^{-1.025\sqrt{\Phi}d} \quad \text{where } [d] = \text{\AA}; [\Phi] = \text{eV};$$

With 5eV as typical example for a workfunction value a change of 1Å in distance causes a change of nearly one order of magnitude in current. This facilitates the high vertical resolution.

Also

$$I \propto V \rho_{sa}(d, E_F),$$

which means that the current is proportional to the local density of states of the sample at the Fermi energy at a distance d , i.e. the position of the tip.

A more exact calculation of the current density of the square barrier problem requires the Schrödinger's equation to be solved in the three regions: before, in and behind the barrier. The coefficients have to be adapted so that the overall solution is continually differentiable. Defining the transition probability as

$$T = \frac{j_T}{j_i}$$

yields

$$T = \frac{16E(V-E)}{V^2} e^{-2\kappa d}; \quad \kappa = \sqrt{\frac{2m(V-E)}{\hbar^2}}$$

with the approximation $\kappa d \gg 1$.

The current density itself is defined as

$$j_z = -\frac{i\hbar}{2m} \left(\Psi^*(z) \frac{d\Psi}{dz} - \Psi(z) \frac{d\Psi^*}{dz} \right)$$

For a nonsquare potential the WKB method must be used. This is more adequate as the potential is changed by the applied voltage and influenced by the image force on the electron. The WKB method yields a transition probability of

$$T(E) \propto \exp\left(-\frac{2}{\hbar} \int_0^1 \sqrt{2mV(z) - E} dz\right)$$

Bardeen (quantum) approach to tunneling

2.2. Bardeen Approach

Another way of describing electron tunneling comes from Bardeen's approach which makes use of the time dependent perturbation theory. The probability of an electron in the state Ψ at E_Ψ to tunnel

into a state χ at E_χ is given by Fermi's Golden Rule

$$w = \frac{2\pi}{\hbar} |M|^2 \delta(E_\Psi - E_\chi)$$

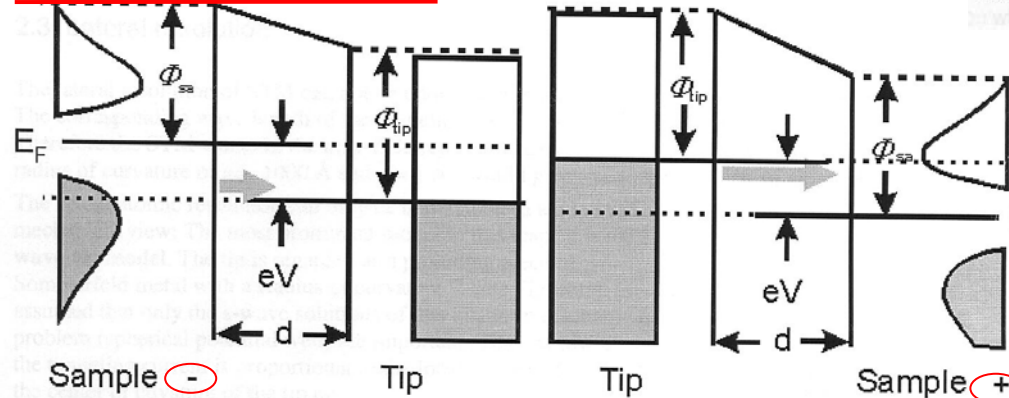
The tunneling matrix element is given by an integral over a surface in the barrier region lying between the tip and the sample:

$$M = \frac{\hbar}{2m} \int_{z=z_0} \left(\chi^* \frac{\partial \Psi}{\partial z} - \Psi \frac{\partial \chi^*}{\partial z} \right) dS$$

Applying a bias voltage V and approximating the Fermi distribution as a step function ($kT \ll \Delta E_{\text{resolution}}$), the current is

$$I = \frac{4\pi e}{\hbar} \int_0^{eV} \rho_{\text{sa}}(E_F - eV + \varepsilon) \rho_{\text{tip}}(E_F + \varepsilon) |M|^2 d\varepsilon \quad (**)$$

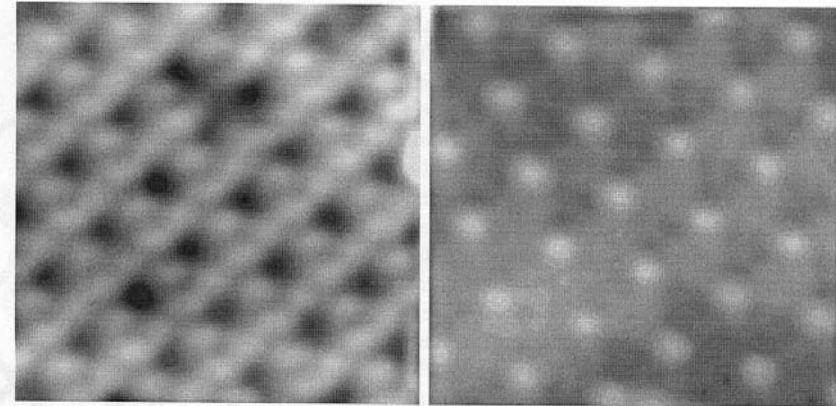
Hence the current is given by a combination of the local densities of states of the sample and the tip, weighted by the tunneling matrix element M .



Schematic of electron tunneling with respect to the density of states of the sample.

$\delta(E_\Psi - E_\chi)$ means that an electron can only tunnel if there is an unoccupied state with the same energy in the other electrode (thus inelastic tunneling is not treated). In case of a negative potential on the sample the occupied states generate the current, whereas in case of a positive bias the unoccupied states of the sample are of importance. Therefore, as shown below, by altering the voltage, a complete different image can be detected as other states contribute to the tunneling current. This is used in tunneling spectroscopy. It should finally be mentioned that the probability of tunneling (expressed by M^2) is larger for electrons which are close to the fermi edge due to the lower barrier.

**Quantum mech.
Treatment**



Imaging the occupied states of SiC(0001)3x3

Imaging the unoccupied states of SiC(0001)3x3

Tunneling current involves both local density of states (of tip and saample) and tip distance

Holes can also tunnel!

Lateral resolution in STM

2.3. Lateral resolution

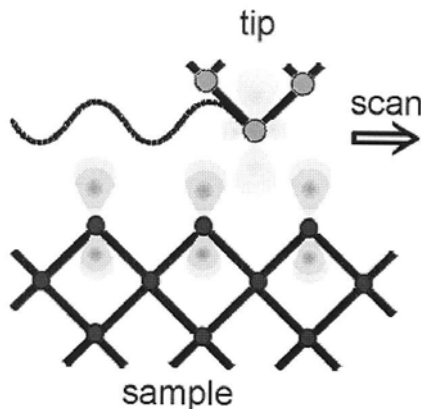
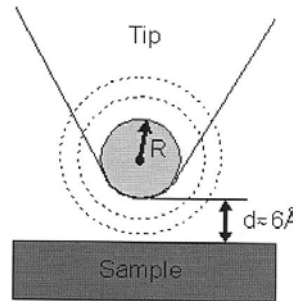
The lateral resolution of STM can not be understood in terms of a Fraunhofer diffraction resolution. The corresponding wave length of the tunneling electron would be $\lambda > 10 \text{ \AA}$.

Therefore the STM works in the near-field regime. The overall geometric curvature of the tip with a radius of curvature of e.g. 1000 \AA and $\kappa = 1 \text{ \AA}^{-1}$ would give rise to a resolution of about 50 \AA .

The actual atomic resolution can only be understood in a quantum mechanical view: The most prominent model in this respect is the **s-wave-tip model**. The tip is regarded as a protruding piece of Sommerfeld metal with a Radius of curvature R (see Figure). It is assumed that only the s-wave solutions of this quantum mechanical problem (spherical potential well) are important. Thus, at low bias the tunneling current is proportional to the local density of states at the center of curvature of the tip r_0 :

$$I \propto \sum_{E_k = E_f - eV}^{E_f} |\Psi_{\mu}(r_0)|^2 = eV \rho_{sa}(r_0, E_f)$$

In this model only the properties of the sample contribute to the STM image which is quite easy to handle. But it cannot explain the atomic resolution.



Interaction which causes a high corrugated tunneling distribution

Calculations and experiments showed that there is often a d_z^2 like state near the fermi edge present at the apex atom which also predominantly contributes to the tunneling current. It is understood that this state (and also the p_z like state) is advantageous for a „sharp, tip. Since the tunneling current is a convolution of the tip state and the sample state, there is a symmetry between both: By interchanging the electronic state of the tip and the sample state, the image should be the same (reciprocity principle). This can also explain the fact that the corrugation amplitude of an STM image is often larger than that of the LDOS of the sample (measured by helium scattering). In this case the tip traces a fictitious surface with a d_z^2 like state. The state of the tip atom is dependent on the material and the orientation. As the tip is quite difficult to handle, it is one of the most difficult problems in a STM experiment.

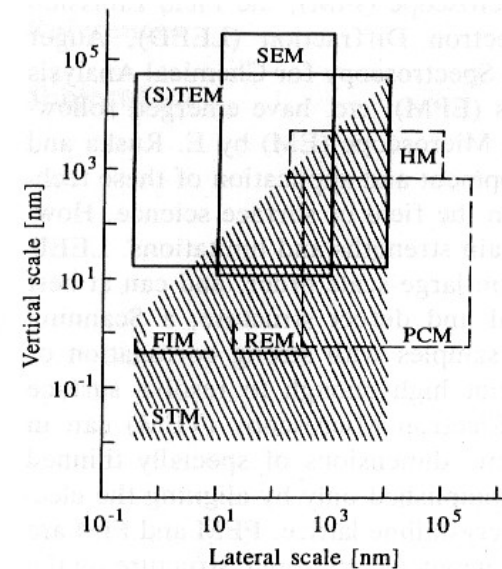


Fig. 1.1. Comparison of the resolution range of STM with that of other microscopes [1. 1]. [HM: High-resolution optical Microscope. PCM: Phase Contrast Microscope. (S)TEM: (Scanning) Transmission Electron Microscope. FIM: Field Ion Microscope. REM: Reflection Electron Microscope]

“Atomic” resolution achievable in STM

Tunneling current and STM

2.1 Theoretical Fundamentals of the Scanning Tunneling Microscope

How does a measuring instrument function that allows us to see single atoms? In the case of a scanning tunnelling microscope a fine metallic tip is used as the probe (called tunnelling tip) (see Figure 3). This tip is approached toward the surface until a current flows when a voltage is applied between the tip and the sample surface. This happens at distances in the order of 1 nm. The current is called tunnel current since it is based on the quantum-mechanical tunnel effect. After a tunnelling contact is established, the tip is moved over the surface by a piezoelectric scanning unit, whose mechanical extension can be controlled by applying appropriate voltages. The scanning unit is typically capable of scanning an area of a few nm up to several μm . This allows us to obtain a microscopic image of the spatial variation of the tunnel current. Hence the name scanning tunnelling microscope.

- A metallic tip is moved as probe towards a conducting surface up to a distance of about 1 nm
- With an applied voltage a current flows due to the tunnel effect (tunnel current)
- The spatial variation of the tunnel current is measured by scanning over the sample surface
- A microscopic image of the surface is produced

At this stage we have to ask what kind of atomic-scale structures can be made visible by the scanning tunnelling microscope utilising the tunnel effect? These structures must by nature correspond to electrical states from or into which the electrons can tunnel. In the tunnelling process, the electrons must tunnel through the vacuum barrier between tunnelling tip and sample, which represents a potential barrier. The tunnel effect allows a particle (here an electron) to tunnel through this potential barrier even though the electron's energy is lower than the barrier height. The probability of such a process decreases exponentially with the geometrical distance between the tip and the sample and with increasing barrier height. An experimental apparatus making use of the tunnel effect must therefore minimise the potential barrier to be tunnelled through. This is realised in the scanning tunnelling microscope configuration by moving the tip very close (about 1 nm) to the surface. The electrons can then pass between the surface and the tip. The direction of the tunnel current is fixed by applying a voltage between sample and tip.

In order to explain and interpret the images of the surface states obtained in this way, efforts to develop a theory were made very soon after the invention of the scanning tunnelling microscope. One of the possible theoretical approaches is based on Bardeen's idea of applying a transfer Hamiltonian operator to the tunnelling process [2]. This had the advantage of adequately describing the many-particle nature of the tunnel junction. In the model, a weak overlap of the wave functions of the surface states of the two electrodes (tunnelling tip and sample surface) is assumed to allow a perturbation calculation. On this basis, Tersoff and Hamann developed a simple theory of scanning tunnelling microscopy [3], [4] Hence follows the tunnel current:

$$I \sim V \cdot \rho_{\text{tip}}(W_F) \cdot \rho_{\text{sample}}(r_0, W_F) \quad (1)$$

The tunnelling tip is assumed to be a metallic s-orbital as shown schematically in Figure 4. In addition, it is assumed that low voltages V (i.e., much smaller than the work function) are applied. $\rho_{\text{tip}}(W_F)$ is the density of states of the tip and $\rho_{\text{sample}}(r_0, W_F)$ is that of the sample surface at the centre r_0 of the tip orbital and at the Fermi energy W_F . Eq. (1) shows that at low voltage the scanning tunnelling microscope thus images the electronic density of states at the sample surface near the Fermi energy. However, this result also means that the scanning tunnelling microscope images do not directly show the atoms, but rather the electronic states bound to the atoms. As can be seen in Eq. (1), the tips density of states enters in the measurement in the same way as the density of states of the sample. It is therefore desirable to know the exact electronic state of the tip, but unfortunately, in practice, every tip is different and the details remain unknown.

- Weak overlap of the wave functions of the surface states of the two electrodes (tunnelling tip and sample surface)
- Tunnelling tip approximated as an s-orbital
- Low voltages ($V \ll$ work function)

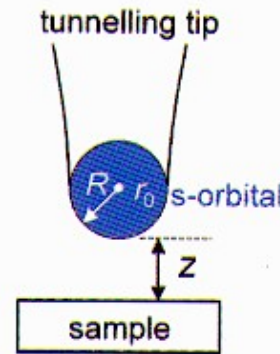


Figure 4: Schematic representation of the tunnelling geometry in the Tersoff-Hamann model.

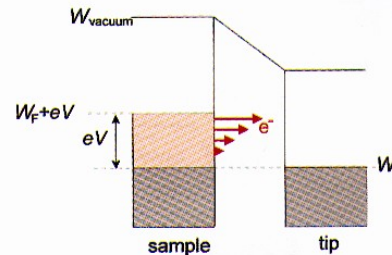


Figure 5: At high voltages not only the states near the Fermi energy W_F contribute to the current but all states whose energy ranges between W_F and $W_F + eV$.

Extension to "high" bias

- The tunnel current is proportional to the local density of states of the sample
- The scanning tunnelling microscope images the electronic local density of states of the sample near the Fermi energy.

In a first approximation the density of surface states decreases exponentially into the vacuum with the effective inverse decay length k_{eff}

$$k_{\text{eff}} = \sqrt{\frac{2m_e B}{\hbar^2} + |k_{\parallel}|^2} \quad (2)$$

m_e is the electron mass and k_{\parallel} is the parallel wave vector of the tunnelling electrons. B is the barrier height, which is approximately a function of the applied voltage V and the work functions Φ_{sample} and Φ_{tip} of the sample and tip [5], respectively:

$$B = \frac{\Phi_{\text{tip}} + \Phi_{\text{sample}}}{2} - \frac{|eV|}{2} \quad (3)$$

The tunnel current thus decreases exponentially with the tip-sample distance z :

$$I \sim \exp[-2k_{\text{eff}} z] \quad (4)$$

The exponential current-voltage dependence is quite essential for the high measurement accuracy of a scanning tunnelling microscope, since even small changes in distance may cause a large change in the tunnel current. Thus the tip just needs one microtip, which is only about 0.1 nm closer to the surface than the next one, and still all current flows over only the closest microtip. Thus even apparently wide tips can yield atomic resolution via one microtip.

The description of the tunnel current by Eq. (1) however, has an important restriction: it strictly speaking only applies to low voltages V . In particular for the investigation of semiconductor surfaces voltages of the order of 2 to 3 V are required due to the existence of a band gap. Thus the theory must be extended. The simplest extension yields:

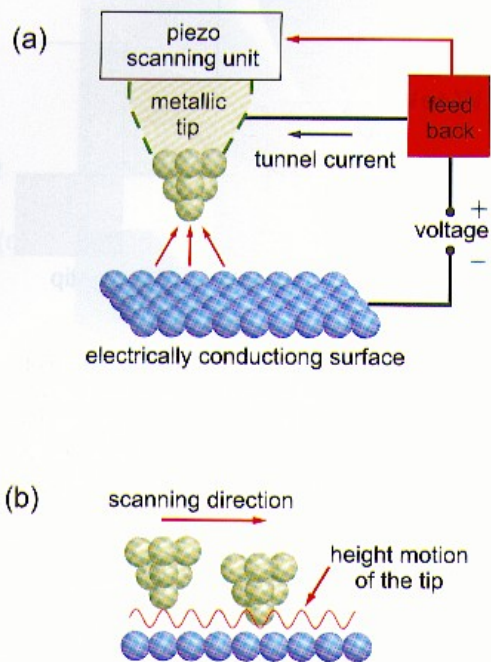
$$I \sim \int_{W_{F,\text{tip}}}^{W_{F,\text{tip}} + eV} \rho_{\text{tip}}(W) \rho_{\text{sample}}(W + eV) T(W, V) dW \quad (5)$$

$T(W, V)$ is a transmission coefficient which depends on the energy of the electrons and the applied voltage. The tunnel current is composed of the product of the density of states of the tip and sample at all the different electron energies that are allowed to participate in the tunnelling process (Figure 5). For example, an image measured at -2 V applied to the sample, consequently shows all occupied sample states with an energy between the Fermi energy and 2 eV below the Fermi energy. Tunnelling at a positive voltages analogously provides a measurement of the empty surface states in an energy interval determined again by the voltage.

In order to illustrate this effect more clearly, in the following the InP(110) surface will be presented. On InP(110) surfaces two electrical states exist near the surface: an occupied state below the valence band edge and an empty state above the conduction band edge (Figure 6). All the other states are located geometrically deeper in the crystal or energetically deeper in the bands. They thus contribute little to the tunnel current.

Da R. Waser Ed., Nanoelectronics and information technology (Wiley-VCH, 2003)

Modes of operation in STM



Constant current

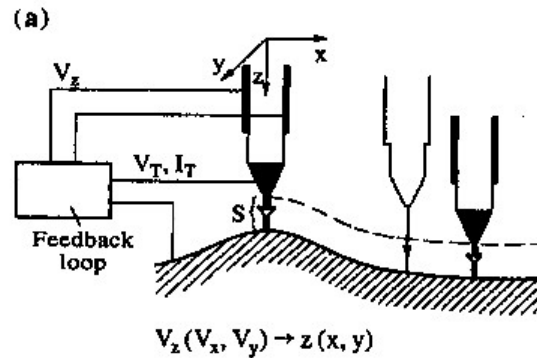


Fig. 1.2a, b. Schematic view of two modes of operation in STM [1.10]. S is the gap between the tip and the sample, I and V_T are the tunneling current and bias voltage, respectively, and V_z is the feedback voltage controlling the tip height along the z direction. (a) constant-current mode and (b) constant-height mode

2.2 Operating Modes of the Scanning Tunneling Microscope

Up to now, the theoretical background of a scanning tunnelling microscope has been presented, but nothing has been said about the experimental operation of a scanning tunnelling microscope. The simplest way to obtain a scanning tunnelling microscope image is to directly measure the variation of the tunnel current as a function of the scanning position while keeping the distance between tip and sample surface constant. A so-called current image is then obtained. Instead of directly recording the atomic variation of the current, however, the usual procedure is to keep the tunnel current constant while scanning over the surface. This is done by changing the distance between tip and surface using a feedback loop (Figure 8). In order to get an image, the voltage required at the piezoelectric crystal to adjust the distance is recorded. One obtains a so-called constant-current STM image.

Feedback loop used to keep constant the tunneling current → “absolute” topography map

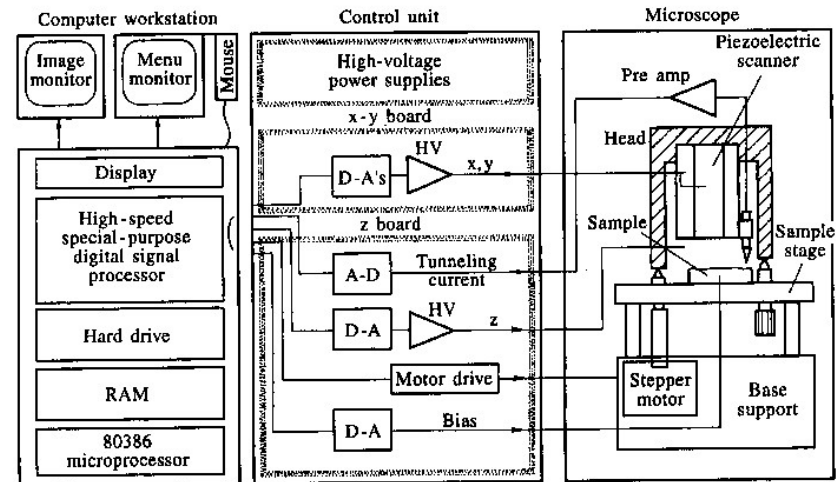


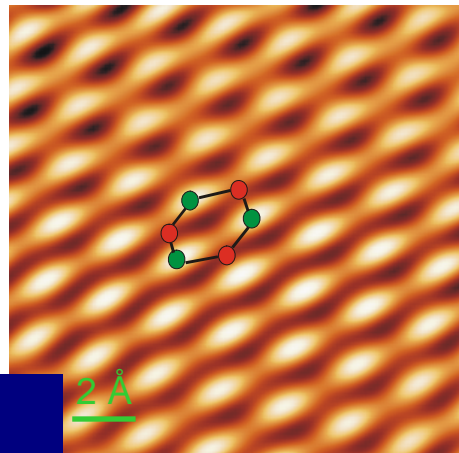
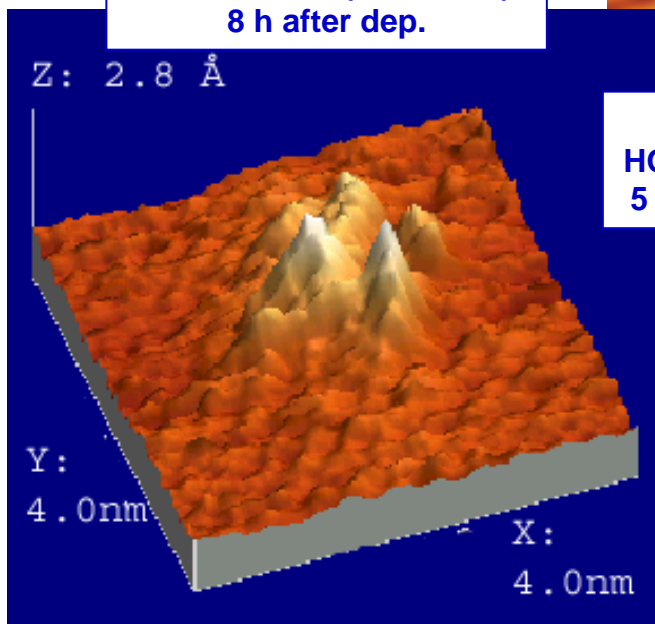
Fig. 4.27. Block diagram of the STM control, data acquisition and display system indicating all of the equipment connections

Atomic resolution in STM

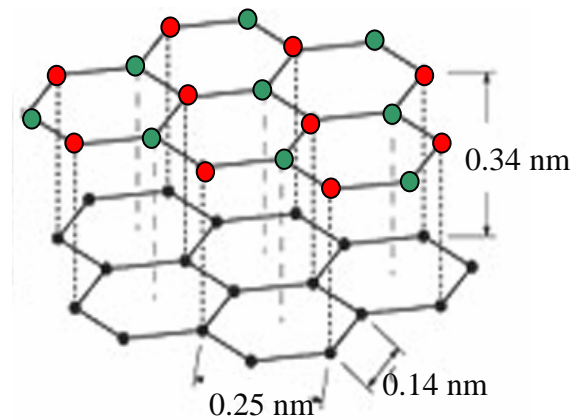
Highly Oriented Pyrolytic Graphite (HOPG) substrates well suited as test samples

A few examples

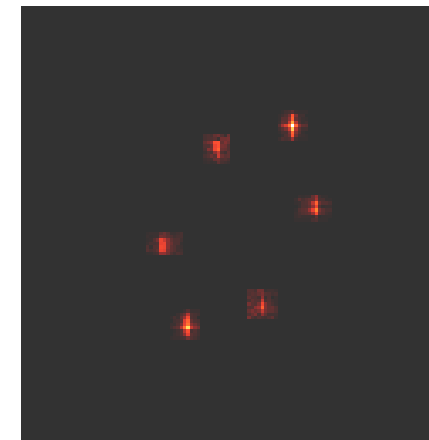
STM image - 3D view
Cs on HOPG (bias 0.5 V)
8 h after dep.



STM image – plan view
HOPG substrate, $p < 10^{-8}$ mbar
5 nm x 5 nm scan (bias 0.5 V)



Surface electron-related features can be easily observed



2D-FFT

Bias polarity-related contrast mechanisms

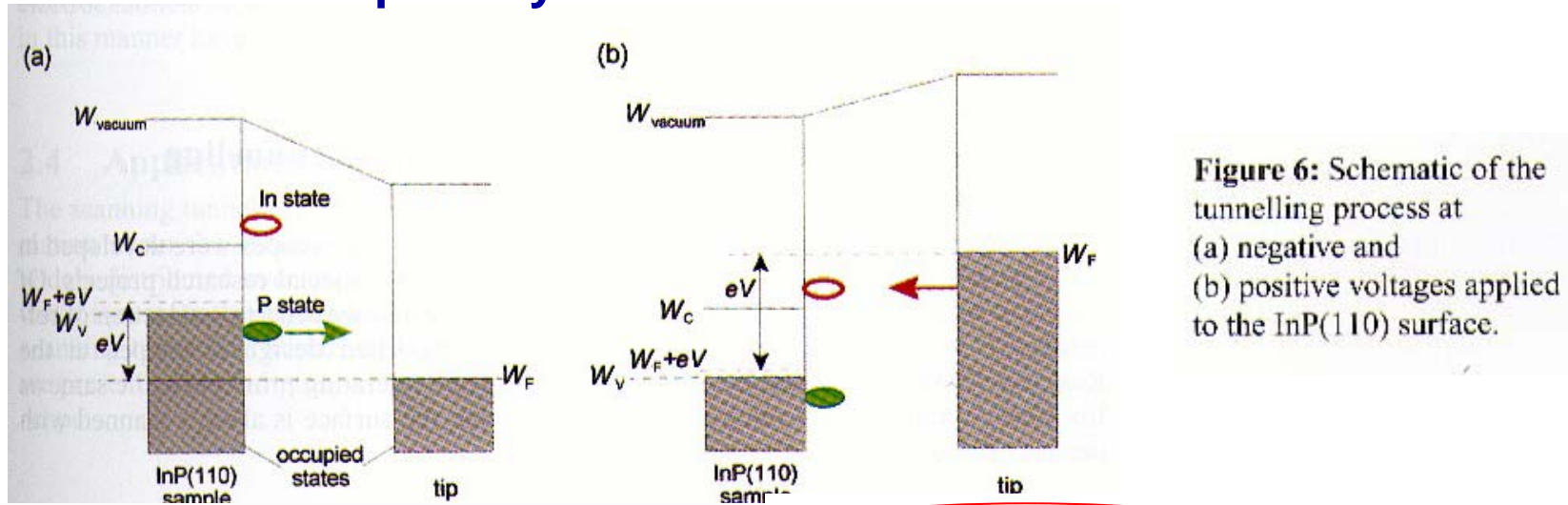


Figure 6: Schematic of the tunnelling process at (a) negative and (b) positive voltages applied to the InP(110) surface.

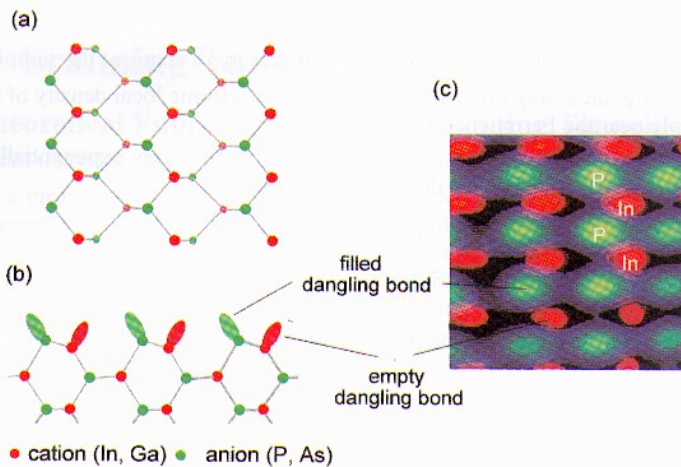


Figure 7:
 (a) Schematic top view and (b) side view of the (110) surfaces of III-V compound semiconductors.
 (c) Superposition of two scanning tunnelling microscope images measured at positive (red) and negative (green) voltage. The density of state maxima correspond to the surface states at the In and P atoms, respectively.

In the special case of the InP(110) surface, the occupied surface state is spatially located above the P atoms, whereas the empty state is bound to the In atoms (Figure 7a,b). The P and In atoms are alternately arranged in zigzag rows. At negative sample voltages, the scanning tunnelling microscope probes the occupied states located at the P sublattice, whose electrons tunnel into the empty states of the tunnelling tip (Figure 6a). Conversely, only the empty surface states at the In sublattice are probed at positive voltages applied to the sample (Figure 6b) [6] – [8]. If the voltage polarity is changed every scan line, i.e. the occupied and the empty states are probed each alternating scan line, the two resulting images can be superimposed and the zigzag rows of alternating "In" and "P" atoms become visible (Figure 7c).

Apart from the spatial distribution of the density of states, its energy dependence is also of interest, and it should be possible to determine this dependence from current-voltage characteristics using Eq. (5). In order to do so, however, information is required about the transmission coefficient, which turns out to be a great obstacle even if approximations [9] are used. Therefore, in most cases, an experimentally viable approach is used, in which the density of states is approximated as follows [10], [11]:

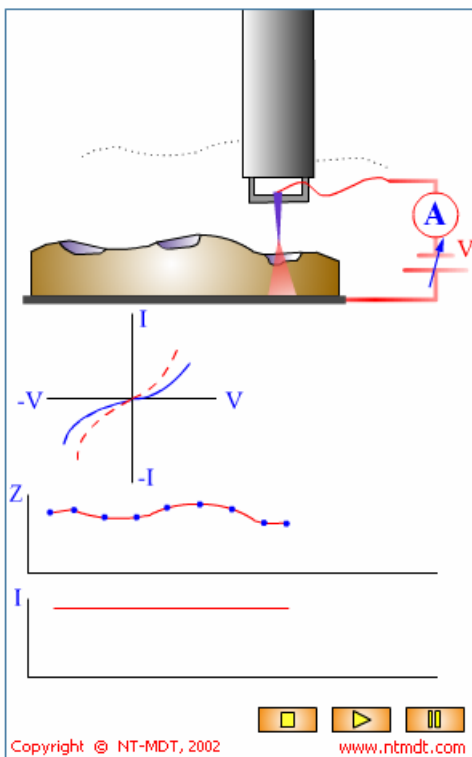
$$\rho_{\text{sample}}(eV) \approx (dI/dV)/(IV) \quad (6)$$

It is thus possible to experimentally measure the density of states as a function of the energy relative to the Fermi level.

Contrast mechanisms related to bias polarity

STM spectroscopy I

I(V) Spectroscopy.



In I(V) Spectroscopy (or Current Imaging Tunneling Spectroscopy, CITS) a normal topographic image is acquired at fixed I_0 and V_0 . At each point in the image feedback loop is interrupted and the bias voltage is set to a series of voltages V_i and the tunneling current I_i is recorded. The voltage is then returned to V_0 and the feedback loop is turned back on. Each I-V spectra can be acquired in a few milliseconds so there is no appreciable drift in the tip position. This procedure generates a complete current image $I_i(x,y)$ at each voltage V_i in addition to the topographic image $z(x,y)|_{V_0}$.

CITS data can be used to calculate a current difference image

$\Delta I_{V_i, V_j}(x,y)$ where V_i and V_j bracket a particular surface state, producing an atomic resolved, real space image of a surface state. This technique, for example can be used in UHV to image filled ad-atom states or the dangling bond states for silicon reconstructions.

References

1. G. Binnig and H. Rohrer: Surf. Sci. 126 (1983) 236. Rep. Prog. Phys. 55, 1165-1240 (1992).

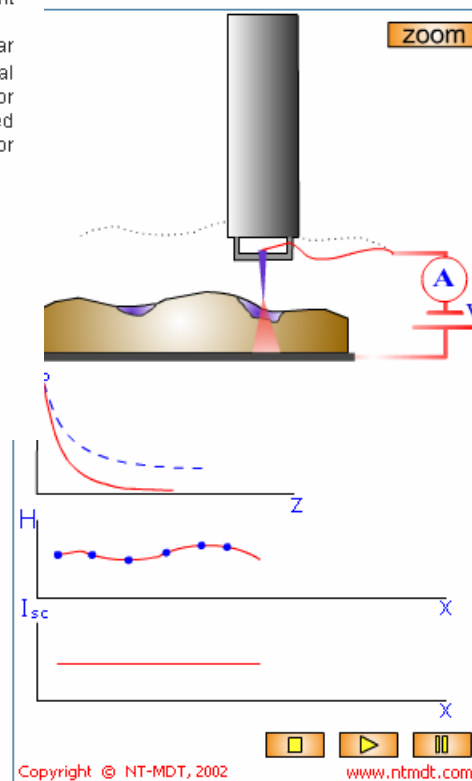
Download [Flash model](#)

Copyright © NT-MDT, 2002

www.ntmdt.com

At one point over the surface, I vs V and I vs Z curves can be acquired

I(z) Spectroscopy.



The $I(z)$ Spectroscopy is related to LBH spectroscopy and can be used for providing an information about the z -dependence of the microscopic work function of the surface. Next important use of the $I(z)$ Spectroscopy is concerned with for testing of the STM tip quality.

The tunneling current I_T in STM exponentially decays with the tip-sample separation z as

$$I_T \sim \exp(-2kz),$$

where the decay constant is given by

$$2k = 2(2mU/h^2)^{1/2}$$

U is the average work function $U_{av} = (U_s + U_t)/2$, where U_t and U_s are the tip and sample work functions, respectively.

In the $I(z)$ Spectroscopy, we measure the tunnel current versus tip-sample separation at each pixel of an STM image. For $U_{av} = 1$ eV $2k = 1.025 \text{ \AA}^{-1} \text{ eV}^{-1}$.

Sharp $I(z)$ dependence helps in determining of tip quality. As is empirically established if tunnel current I_T drop to one-half with $Z < 3 \text{ \AA}$ the tip is considered to be very good, if with $Z < 10 \text{ \AA}$, then using this tip it is possible to have an atomic resolution on HOPG. If this takes place with $Z > 20 \text{ \AA}$ this tip should not be used and must be replaced.

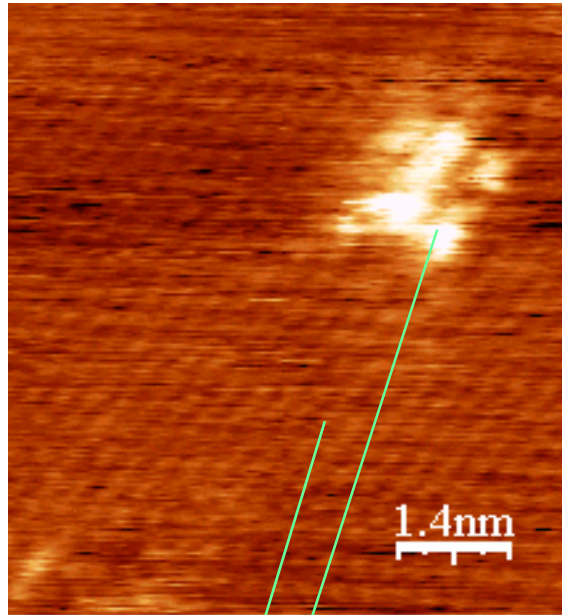
References

Copyright © NT-MDT, 2002

www.ntmdt.com

STM offers analytical tool with unique space resolution capabilities

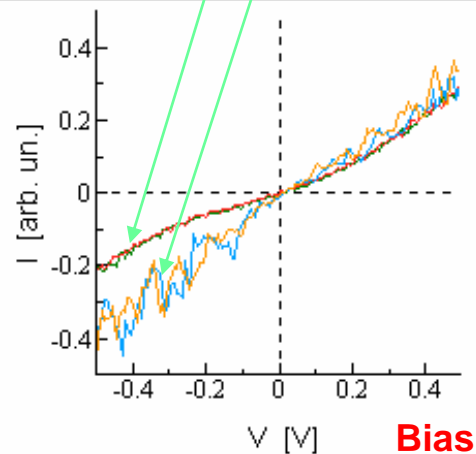
STM spectroscopy II: an example



I-V curves can be acquired at different positions

STM image -
plan view
Cs on HOPG
(bias 0.5 V)
8 h after dep.

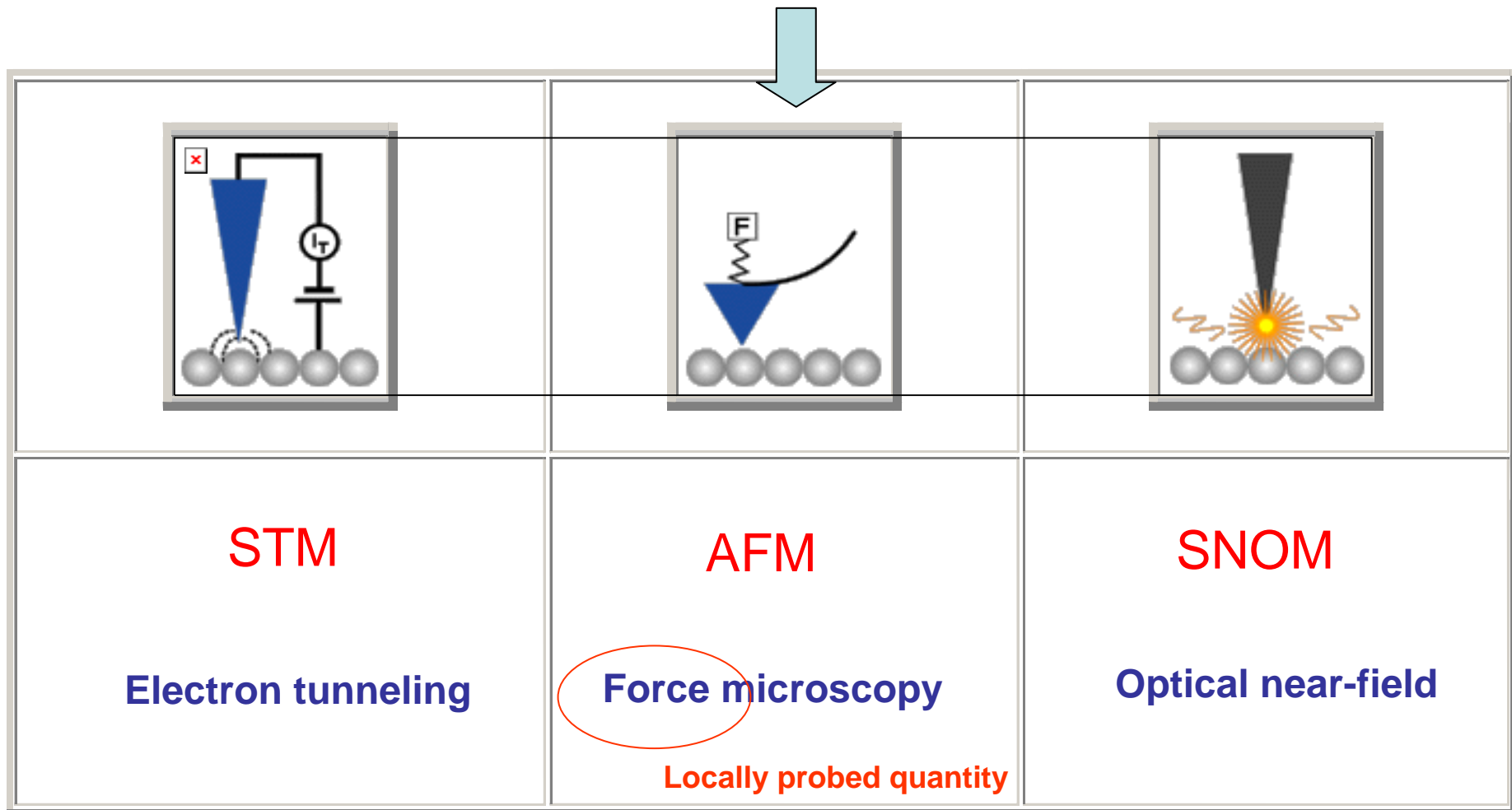
Tunneling
current
(conversion
factor 10^8)



Typical STM I-V
curves of different
regions
(covered/uncovered)

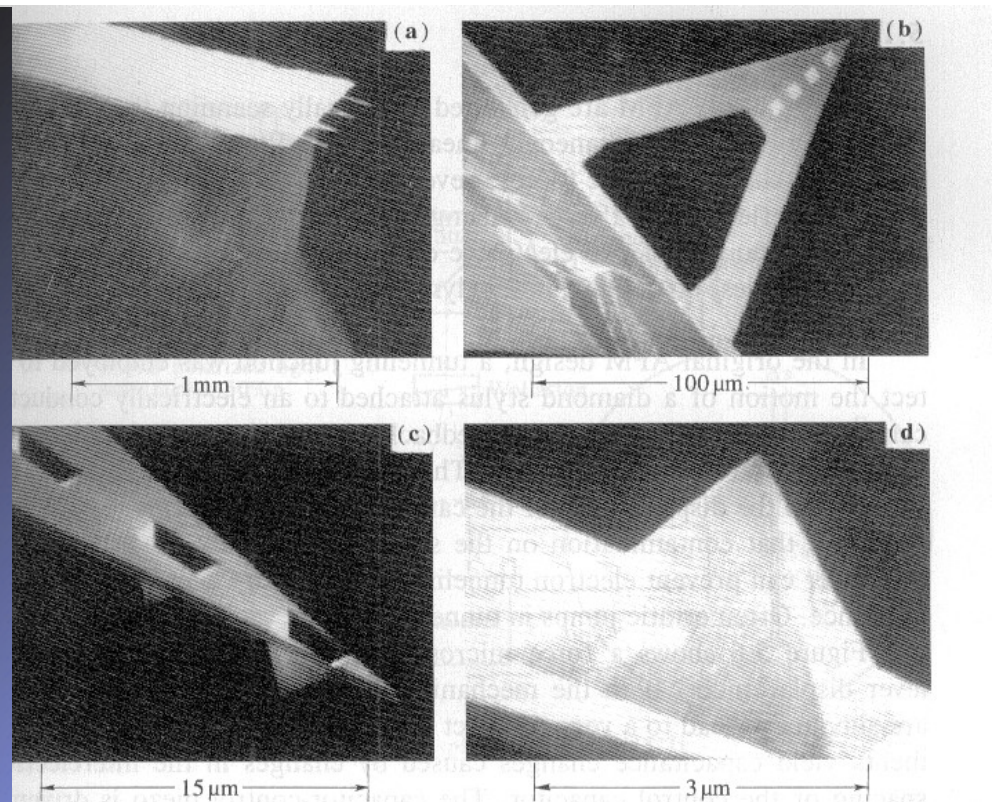
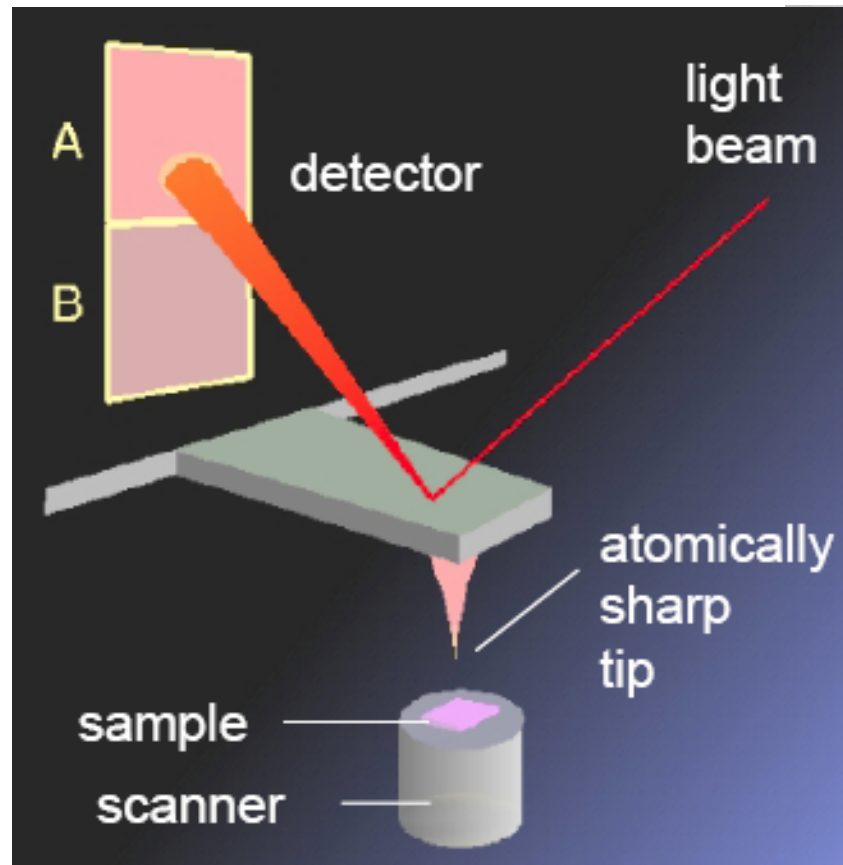
Possibility to discriminate
“conductivity” of small-sized
samples with an excellent
space resolution

2. Scanning force microscopy (AFM and relatives)



AFM is probably the most straightforward (and easy to understand/interpret) probe microscopy

AFM probes



5.5a-d. SEM micrographs of Si_3N_4 cantilevers with integrated pyramidal tips. (a) The Si_3N_4 film is attached to the surface of a glass block with dimensions of $2 \times 3 \times 0.7 \text{ mm}^3$. Four cantilevers protrude from the edge of the block. (b) Four pyramidal tips can be seen at the end of this V-shaped cantilever. (c) The pyramidal tips are hollow when viewed from the back side. (d) Each tip has very smooth sidewalls, and the tip appears to terminate virtually at a point, with less than 30 nm radius [5.4]

The local character of AFM relies on the availability of suitable probes

Cantilever/tip fabrication: examples

The first step in the fabrication of an AFM tip is the etching of a single-crystal silicon wafer with specific crystalline orientation. This results in the forming of square pyramidal tips with characteristic angles.

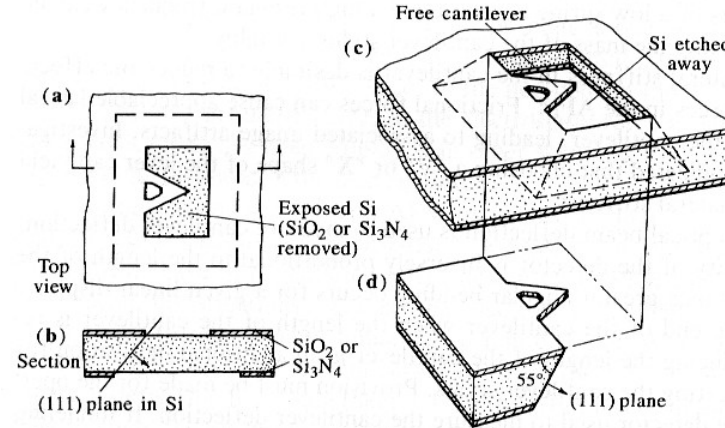
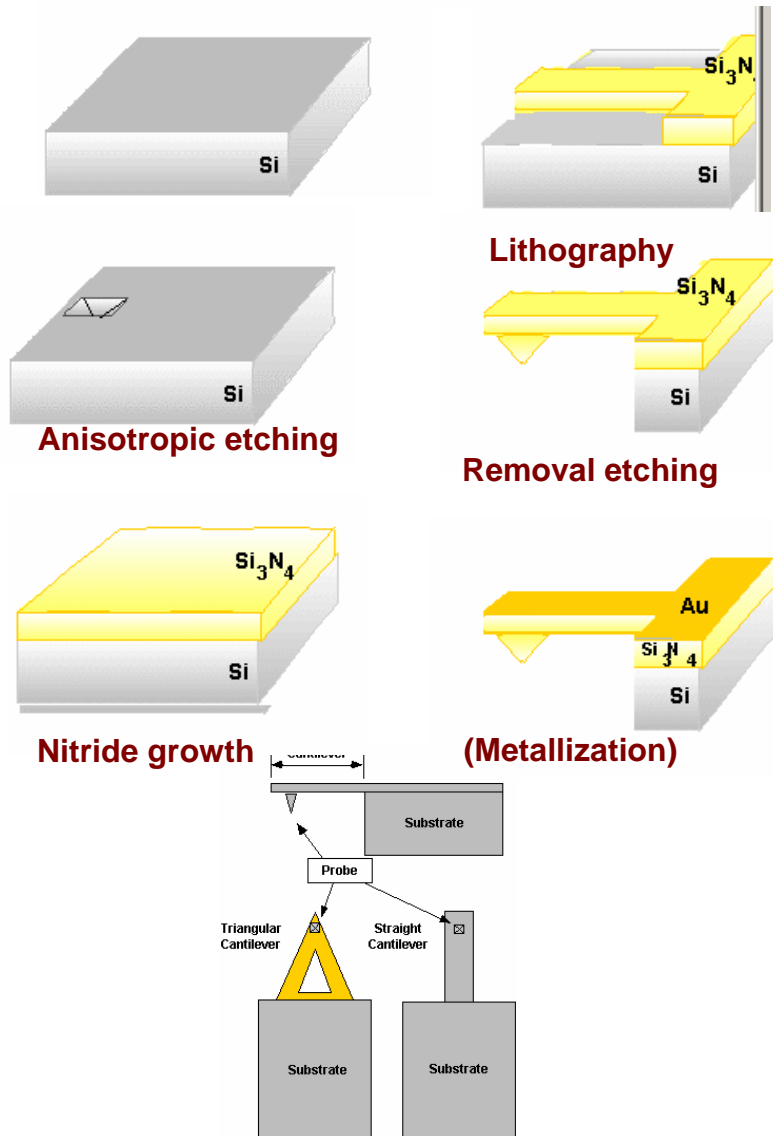


Fig. 5.2a-d. Fabrication of thin-film microcantilevers. (a) A thin film of SiO_2 or Si_3N_4 is formed on the surface of a (100) Si wafer and patterned to define the shape of the cantilever and to create openings on the top and bottom of the wafer. (b) The windows are aligned along (111) planes. (c) Anisotropic etching of the exposed Si with KOH undercuts the cantilever and self-terminates at the (111) planes as shown. (d) A small Si chip is cut from the wafer to serve as a pedestal for mounting the cantilever in the AFM [5.4]

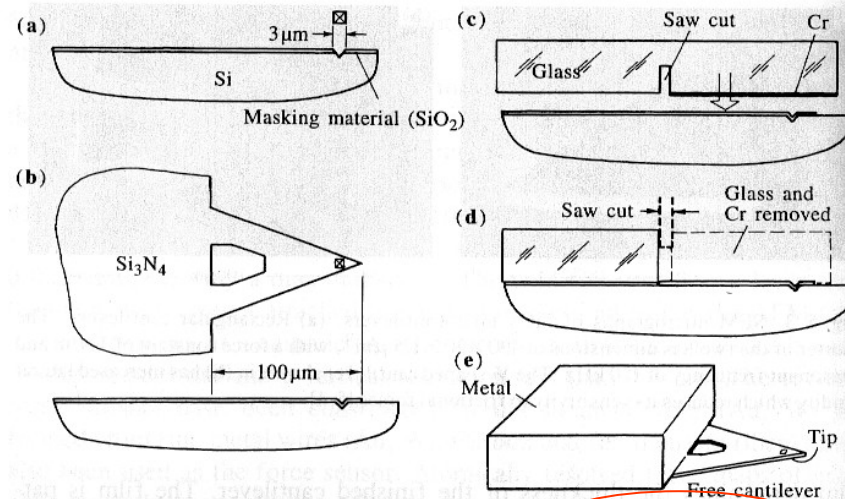
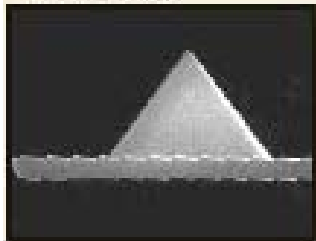


Fig. 5.4a-e. Fabrication of Si_3N_4 microcantilevers with integrated pyramidal tips. (a) to (e) illustrate the steps in the fabrication process, see text [5.4]

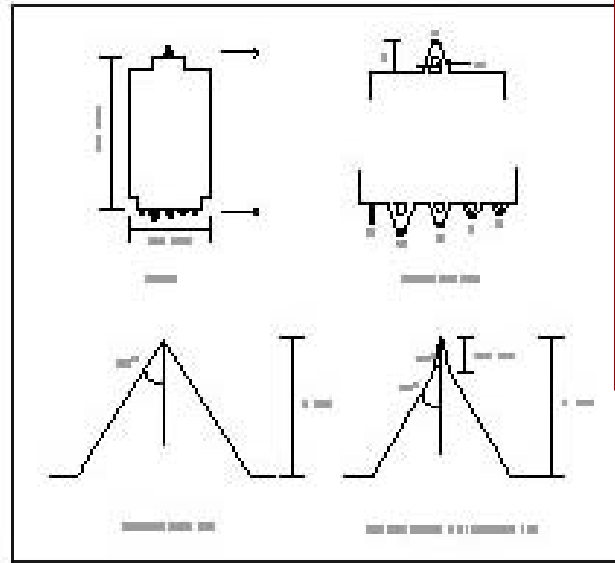
Examples of commercial cantilevers

FEATURES:

- Compatible with all major AFM brands.
- Typical radius of curvature: sharpened tips: < 20 nm, unsharpened tips: < 50 nm.
- Available with gold coating for high reflectivity.
- Recessed corners for easy sample approach.
- The widest range of spring constants commercially available on a single chip.



Thermomicroscopes Microlevers are ideal for all contact imaging modes, force modulation microscopy, and liquid operation. The range in force constants enable users to image soft samples in contact as well as high load force vs. distance spectroscopy.



Many different cantilevers are commercially available

They are different for:

- Dimensions and shape, typ 0.1-0.5 mm;
- Elastic constant (materials and design, typ 0.05-50 N/m;
- Tip coating (conductive, super-hard, etc.)

Typical Mechanical Characteristics

Cantilever type	A - triangular	B - rectangular	C - triangular	D - triangular	E - triangular	F - triangular
Standard mode of operation	Contact					
Cantilever length	180 µm	200 µm	320 µm	220 µm	140 µm	85 µm
Cantilever width	18 µm	20 µm	22 µm	22 µm	18 µm	18 µm
Cantilever thickness	0.6 µm	0.6 µm	0.6 µm	0.6 µm	0.6 µm	0.6 µm
Force Constant	0.05 N/m	0.02 N/m	0.01 N/m	0.03 N/m	0.10 N/m	0.50 N/m
Resonant Frequency	22 kHz	15 kHz	7 kHz	15 kHz	38 kHz	120 kHz

Ordering Information

Microlevers	Sharpened		Unsharpened	
	Gold coated*	Uncoated	Gold coated*	Uncoated
Quantity				
Half wafer - (250 chips)	MSCT-AUHW	MSCT-NGHW	MLCT-AUHW	MLCT-NGHW
Unmounted - (25 chips)	MSCT-AUNM	MSCT-NGNM	MLCT-AUNM	MLCT-NGNM
Mounted - (25 chips)	MSCT-AUMT-A	MSCT-NGMT-A	MLCT-AUMT-A	MLCT-NGMT-A
Mounted - (25 chips)	MSCT-AUMT-BF	MSCT-		F

* Not for use with AutoProbe ME systems

Microlevers™

GENERAL PURPOSE CANTILEVERS

Cantilever choice depends for instance on:

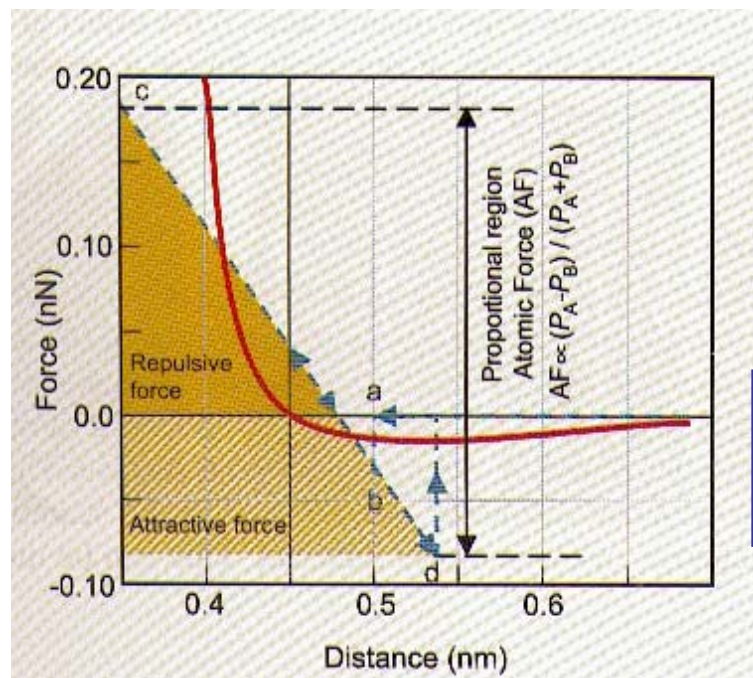
- Operation mode (contact/non contact);
- Quantities to be probed (e.g., if an electric field is needed, a conductive tip has to be used);
- Possible material manipulation (e.g., nanoindentation requires super-hard tips)

Basics of tip/sample interaction

When the tip is approached to the sample (at sub-nm distance!), forces depend roughly on van der Waals interaction between the apical tip atoms and the surface

At “large” distance forces are weakly attractive, at “short” distance they are repulsive

Surface topography (height variations) can be sensed by monitoring the force, i.e., the cantilever deflection



When tip/sample distance is kept in the repulsive region, **contact operating mode** is achieved

When tip/sample distance is kept (*mostly*) in the attractive region, **non-contact operating mode** is achieved

Scanning Force Microscopy

3.2 The Operation Principle of Scanning Force Microscope

The main electronic components of the SFM are the same as for the STM, only the topography of the scanned surface is reconstructed by analysing the deflection of the tip at the end of a spring. Today, the interferometrical and optical lever method dominate commercial SFM apparatus. The most common method for detecting the deflection of cantilever is by measuring the position of a reflected laser-beam on a photosensitive detector. The principle of this optical lever method is presented in Figure 18 a. Without

cantilever displacement both quadrants of the photodiode (A and B) have the same irradiation $P_A = P_B = P/2$ (P represents the total light intensity). The change of the irradiated area in the quadrants A and B is a linear function of the displacement

$$\delta \propto \Delta d = 2 \sin(\Theta) \cdot S_2 = 2\Theta \cdot S_2 = 3S_2 \cdot \delta / L \quad (10)$$

For small angles $\sin(\Theta) \approx \Theta$ and Θ may be evaluated from the relation $\Theta = 3\delta / 2L$ (Figure 18b). For P_A and P_B one would get approximately $P_A = P/2 \cdot (d + \Delta d) / 2$ and $P_B = P/2 \cdot (d - \Delta d) / 2$. Using the simple difference between P_A and P_B would lead to

$\Delta P = P \cdot 3S_2\delta / (Ld)$ but in this case one cannot distinguish between the displacement δ of the cantilever and the variation in the laser power P . Hence the normalised difference is used, which is only dependent of δ :

$$\frac{P_A - P_B}{P_A + P_B} = \delta \cdot \frac{3S_2}{Ld} \quad (11)$$

The "lever amplification" $\Delta d / \delta = 3S_2 / L$ is about a factor of one thousand. On the basis of this kind of technique one is able to detect changes in the position of a cantilever of the order of 0.01 nm.

For large distances between the tip and the sample the bending of the cantilever by attractive forces is negligible. After the cantilever is brought closer to the surface of the sample (point "a" Figure 18c) the van der Waals forces induce a strong deflection of the cantilever and, simultaneously, the cantilever is moving towards the surface. This increases the forces on the cantilever, which is a kind of positive feedback and brings the cantilever to a direct contact with the sample surface (point "b"). However, when the cantilever is brought even closer in contact to the sample, it actually begins to bend in the opposite direction as a result of a repulsive interaction ("b-c"). In the range ("b-c") the position of the laser beam on both quadrants, which is proportional to the force, is a linear function of distance. On reversal this characteristic shows a hysteresis. This means that the cantilever loses contact with the surface at a distance (point "d") which is much larger than the distance on approaching the surface (point "a").

Up to now, the actual probe, i.e. the tip of the leaf spring, has not been discussed in detail. Its preparation is particularly demanding since the tip and the sensitive spring should be one piece. Moreover, the cantilever should be as small as possible. Nowadays, such scanning tips are commercially available (in contrast to the tunnelling tips, which you should prepare yourself). Figure 19 shows such a spring with tip (cantilever) made of Si. The characteristic parameters of a cantilever has been presented in Figure 18b. The spring constant $k = Ead_c^3 / 4L^3 \sim 0.1 - 10 \text{ N/m}$ of the cantilever enables topographical analysis with atomic resolution.

For the realisation of a scanning force microscope, the force measurement must be supplemented by a feedback control, in analogy to the scanning tunnelling microscope. The controller keeps the amplitude of the vibration of the cantilever (the tip), and thus also the distance, constant. During scanning the feedback controller retracts the sample with the scanner of a piezoelectric ceramic or shifts towards the cantilever until the vibration amplitude has reached the setpoint value again. The principle of height regulation is exactly the same as for the scanning tunnelling microscope. The scanning force micrographs thus show areas of constant effective force constant. If the surface is chemically homogeneous and if only van der Waals forces act on the tip, the SFM image shows the topography of the surface.

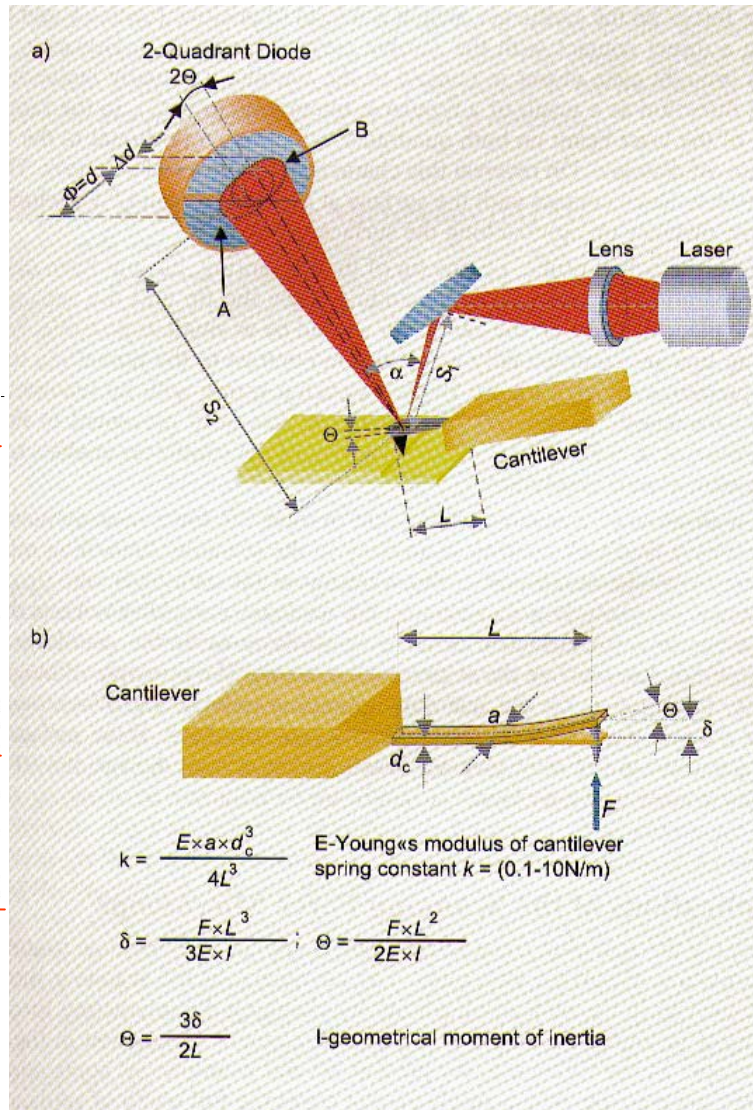


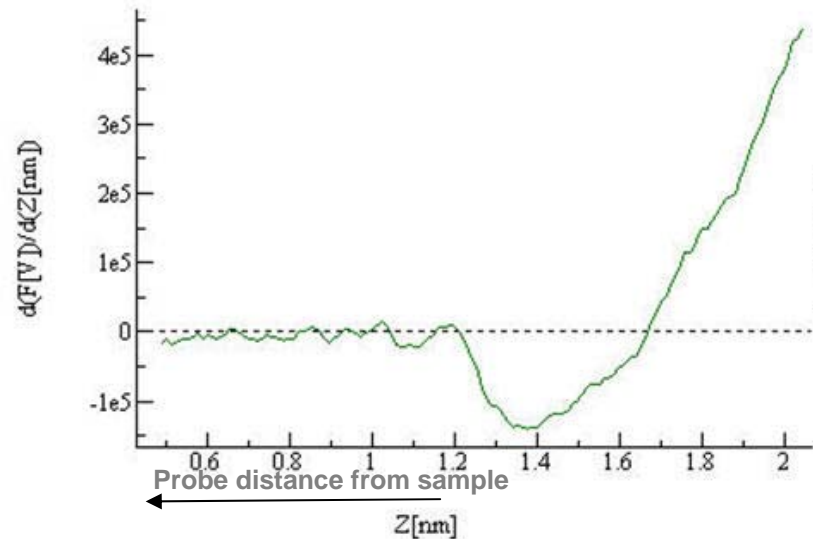
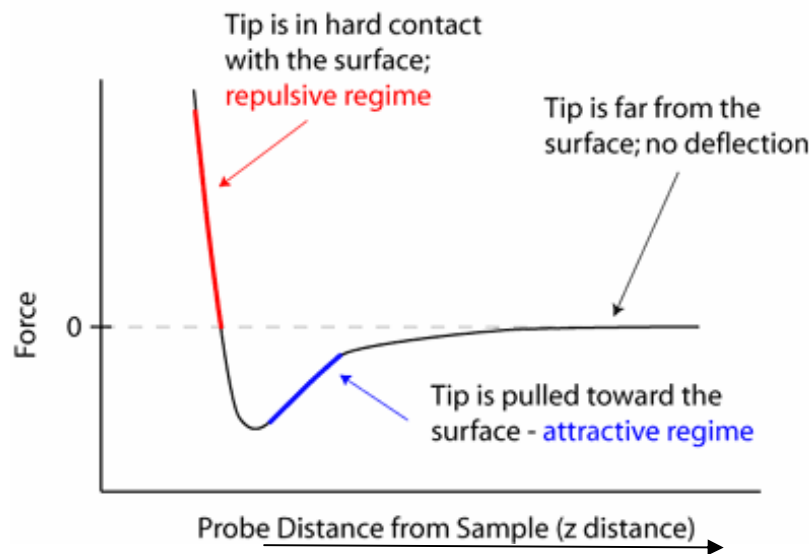
Figure 18: The amplification of the cantilever motion through the optical lever arm method. (a) Optical laser path in the standard AFM set-up. (b) Cantilever beam in bending. (c) Cantilever force as a function of the distance tip – sample distance.

An optical lever method is used to detect the cantilever deflection

Force vs distance curves

In the approaching step, force (i.e., cantilever deflection) vs distance plots have a typical behavior

Force vs distance curves can be used to get local information on the mechanical properties of the surface (*force spectroscopy*)



Note: we are discussing of the **contact mode operation** and tip might penetrate into the sample (*as in nanoindentation – we will see later!*)

Contact mode of operation

3.1 Theoretical Principles of the Scanning Force Microscope

As already mentioned above, van der Waals forces lead to an attractive interaction between the tip on the spring and the sample surface. Figure 15 shows schematically the van der Waals potential between two atoms. The potential can be described in a simpler classical picture as the interaction potential between the time dependent dipole moments of the two atoms. Although the centres of gravity of the electronic charge density and the charge of nucleus are exactly overlapping on a time average, the separation of the centres of gravity is spatially fluctuating in every moment. This produces statistical fluctuations of the atoms' dipole moments. The dipole moment of an atom can again induce a dipole moment in the neighbouring atom and the induced dipole moment acts back on the first atom. This creates a dipole-dipole interaction on basis of the fluctuating dipole moments. This interaction decreases with d^6 in the case of small distances d (Lenard-Jones potential). At larger distances, the interaction potential decreases more rapidly (d^7). This arises from the fact that the interaction between dipole moments occurs through the exchange of virtual photons. If the transit time of the virtual photon between atoms 1 and 2 is longer than the typical fluctuation time of the instantaneous dipole moment, the virtual photon weakens the interaction. This range of the van der Waals interaction is therefore called retarded, whereas that at short distances is unretarded.

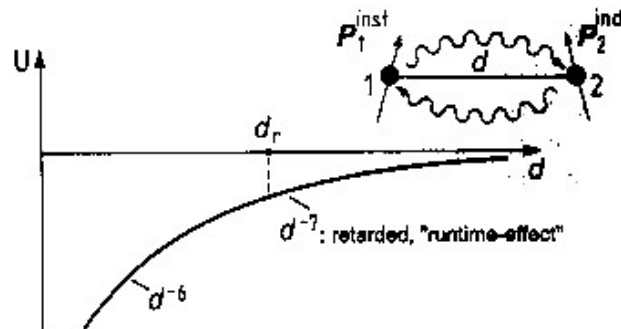


Figure 15: The van der Waals potential U between two atoms. d_r is the critical distance above which the transit time effects weaken the interaction [23].

Contact mode is suitable for rather rigid surfaces

The scanning force microscope is not based on the interaction of individual atom only. Both the sample and the tip are large in comparison to the distance. In order to obtain their interaction, all forces between the atoms of both bodies need to be integrated. The result of this is known for simple bodies and geometries. In all cases, the summation leads to a weaker decrease of the interaction. A single atom at distance d relative to a half-space leads to an interaction potential of

$$U = -\frac{C\pi\rho}{6} \cdot \frac{1}{d^3} \quad (7)$$

where C is the interaction constant of the van der Waals potential and ρ the density of the solid. C is basically determined by the electronic polarizabilities of the atoms in the half-space and of the single atom. If one has two spheres with radii R_1 and R_2 at distance d (distance between sphere surfaces) one obtains an interaction potential of

$$U = -\frac{AR_1R_2}{6(R_1 + R_2)} \cdot \frac{1}{d} \quad (8)$$

where A is the so-called Hamaker constant. It is materials specific and essentially contains the densities of the two bodies and the interaction constant C of the van der Waals potential. If a sphere with radius R has a distance d from a half-space, an interaction potential of

$$U = -\frac{AR}{6} \cdot \frac{1}{d} \quad \text{Realistic tip/surface potential} \quad (9)$$

is obtained from Eq. (8). This case describes the geometry in a scanning force microscope best and is most widely used. The distance dependence of the van der Waals potential thus obtained is used analogously to the distance dependence of the tunnel current in a scanning tunnelling microscope to achieve a high resolution of the scanning force microscope. However, since the distance dependence is much weaker, the sensitivity of the scanning force microscope is lower.

In the contact mode of operation, mechanical interaction leads to tip displacement, i.e., to cantilever deflection related to topography changes

As in STM (constant gap), typical operation foresees a **feedback** system, acting on the Z direction of the piezoscanner, which keeps constant the cantilever deflection during the scan

The "error signal" of the feedback system provides a **topography map (with a calibrated sub-nm space resolution)**

Non-contact mode of operation

The dynamic operation method of a scanning force microscope has proved to be particularly useful. In this method the nominal force constant of the van der Waals potential, i.e. the second derivative of the potential, is exploited. This can be measured by using a vibrating tip (Figure 16). If a tip vibrates at distance d , which is outside the interaction range of the van der Waals potential, then the vibration frequency and the amplitude are only determined by the spring constant k of the spring. This corresponds to a harmonic potential. When the tip comes into the interaction range of the van der Waals potential, the harmonic potential and the interaction potential are superimposed thus changing the vibration frequency and the amplitude of the spring.

This is described by modifying the spring constant k of the spring by an additional contribution f of the van der Waals potential. As a consequence, the vibration frequency is shifted to lower frequencies as shown in Figure 17. ω_0 is the resonance frequency without interaction and $\Delta\omega$ the frequency shift to lower values. If an excitation frequency of the tip of $\omega_m > \omega_0$ is selected and kept constant, the amplitude of the vibration decreases as the tip approaches the sample, since the interaction becomes increasingly stronger. Thus, the vibration amplitude also becomes a measure for the distance of the tip from the sample surface. If a spring with low damping Q^{-1} is selected, the resonance curve is steep and the ratio of the amplitude change for a given frequency shift becomes large.

In practice, small amplitudes (approx. 1 nm) in comparison to distance d are used to ensure the linearity of the amplitude signal. With a given measurement accuracy of 1 %, however, this means that the assembly must measure deflection changes of 0.01 nm, which is achieved most simply by a laser interferometer or optical lever method.

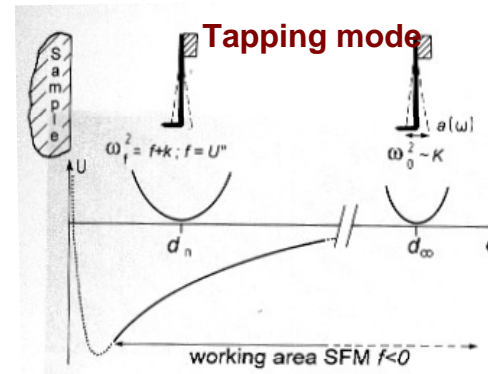


Figure 16: Schematic representation of the effect of the van der Waals interaction potential on the vibration frequency of the spring with tip. As the tip approaches the surface, the resonance frequency of the leaf spring is shifted. (from [23]).

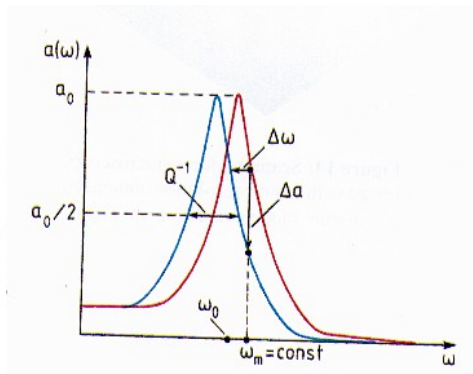


Figure 17: Resonance curves of the tip without and with interaction with a van der Waals potential. The interaction leads to a shift $\Delta\omega$ of the resonance frequency with the consequence that the tip excited with the frequency ω_m has a vibration amplitude $a(\omega)$ attenuated by Δa [23].

In **non-contact (tapping) mode**, the tip/sample distance is continuously modulated thanks to a vibrating tip

Tip vibration is typically achieved by using a piezoelectric transducer fed by an oscillating voltage and mechanically coupled to the cantilever

Oscillation frequency is typically set around the mechanical resonance frequency of the system (cantilever+tip), i.e., hundreds of kHz

The vibration reflects in an oscillation of the position-sensitive detector (multiquadrant diode) and amplitude is monitored

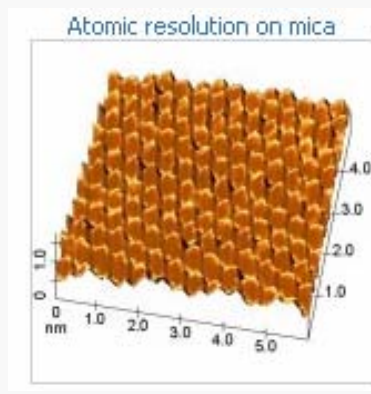
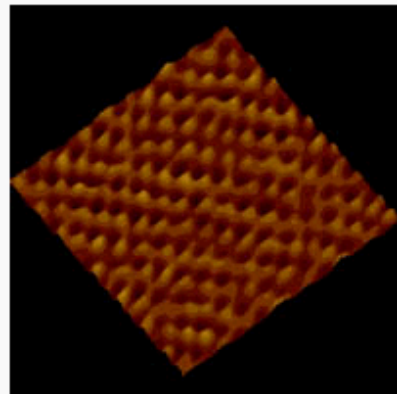
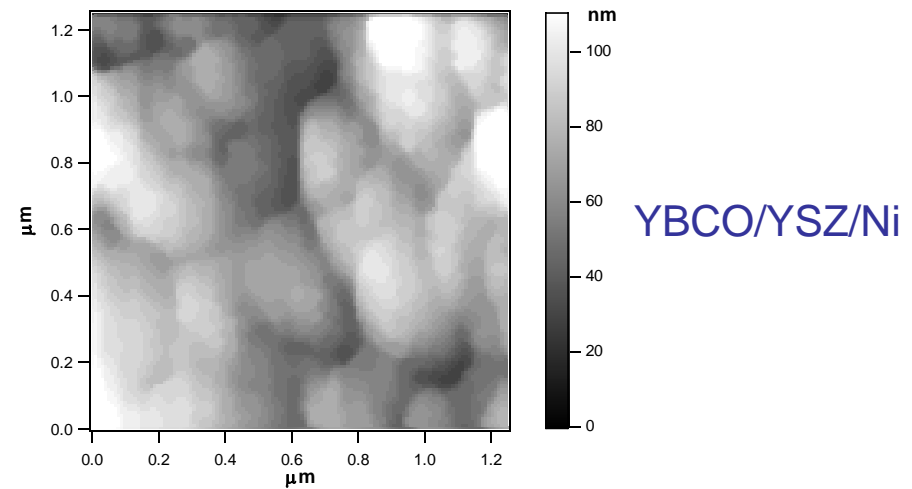
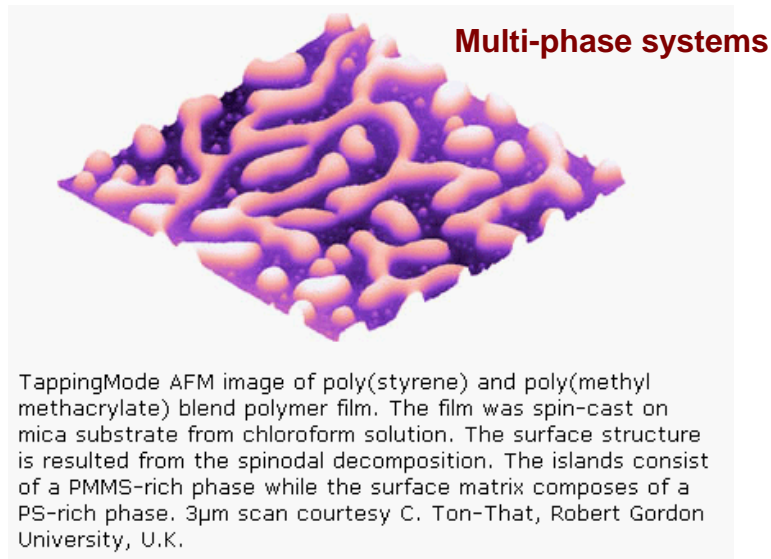
Tip/sample interaction leads to a **damping** (and **phase shift**) of the recorded oscillation when the distance gets small

Suitably conditioned electronic signals are sent into the feedback system in order to stabilize the distance and to derive the topography map

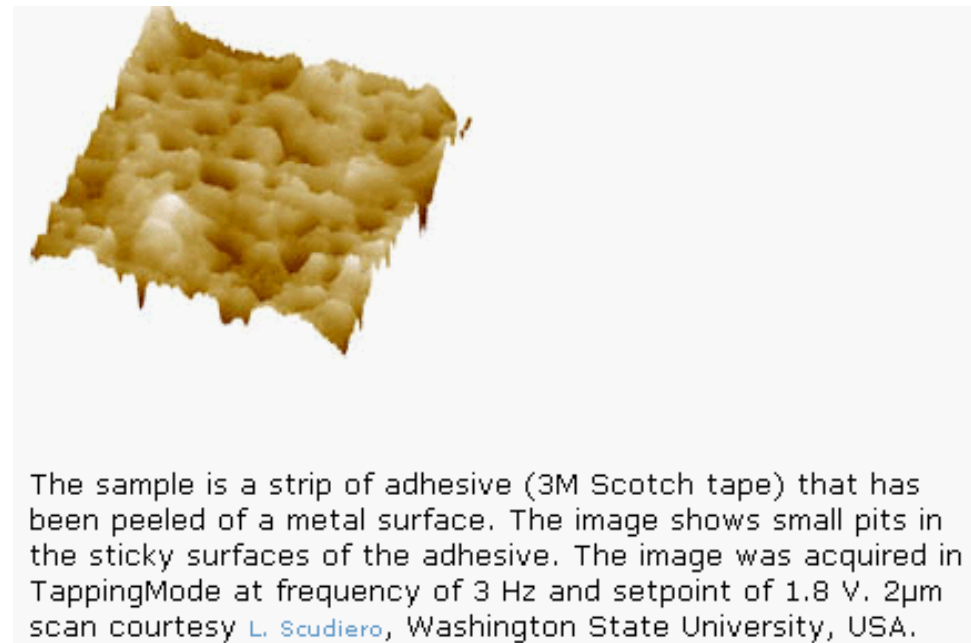
Non-contact modes suitable for "soft" surfaces

No sample preparation is needed!!

A very few examples of AFM images



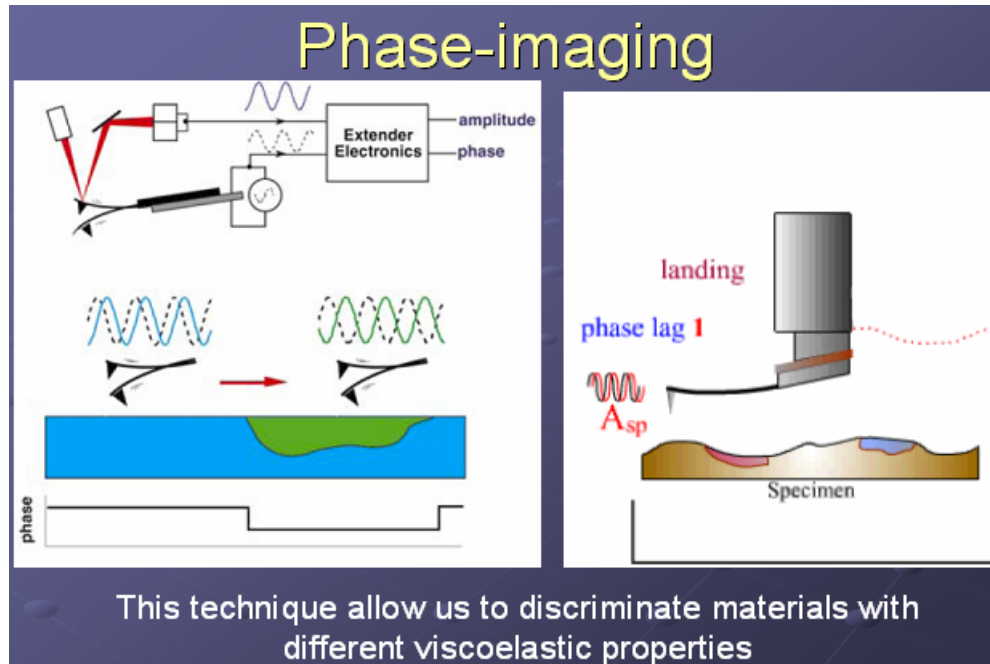
Atomic resolution image of the titanium oxide layer on top of a titanium substrate. Contact mode AFM in air, commercial silicon nitride cantilever. 5 nm scan courtesy P. Cacciafesta, University of Bristol, UK.



See <http://www.veeco.com>

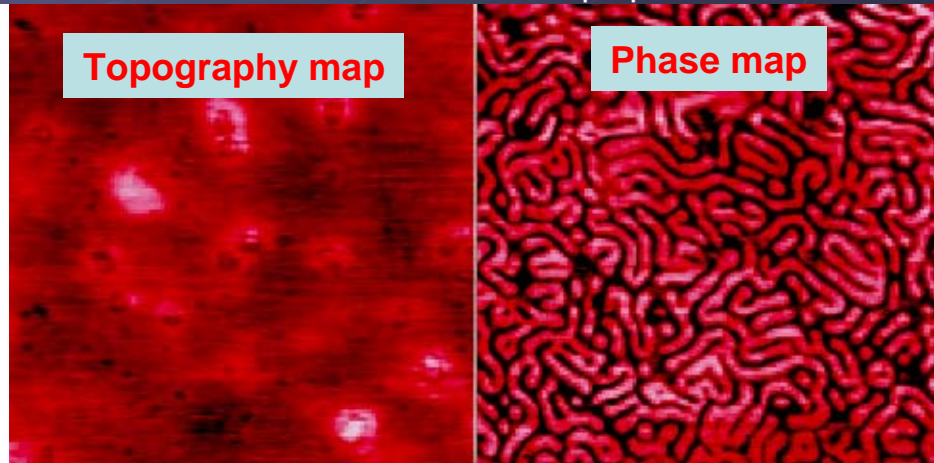
Phase imaging techniques

Animations at www.ntmdt.com!



Dephasing between mechanical oscillation (e.g., the tapping oscillation) and the response of the surface (affecting the tip deflection) depends on the viscoelasticity of the surface (purely elastic vs Newton fluid)

Interpretation similar to a forced and damped mechanical oscillator



Phase imaging:
- adds a contrast mechanism;
- allows for local material analyses

Materiale tratto da seminario PhD di Michele Alderighi, 2005

2.B. Force microscopies derived from AFM

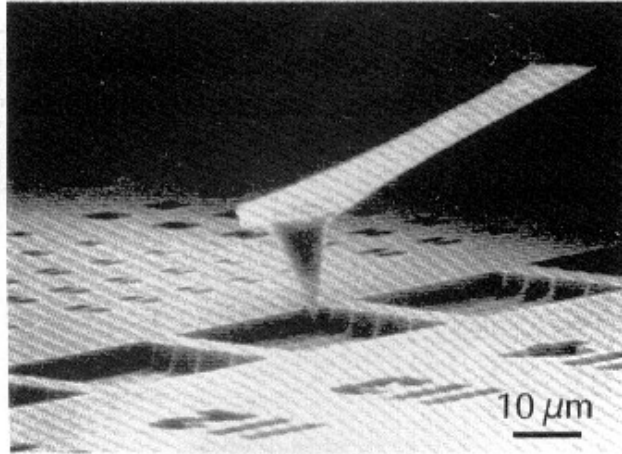


Figure 19: Scanning electron micrograph of a cantilever made of Si. [24].

We have seen how AFM, based on the occurrence of tip/surface van der Waals forces, can map the local topography of the sample

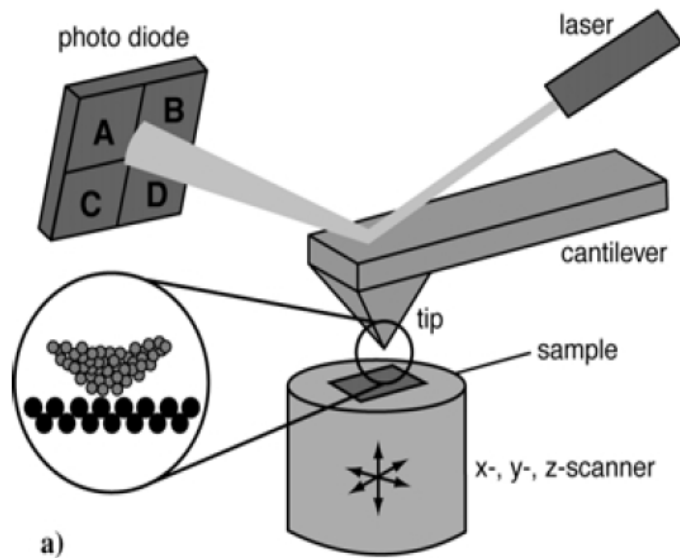
No sample preparation is needed, and the topography map is obtained with “absolute” calibration

The achievable space resolution can reach the **atomic level**, even though most common instruments are capable of a slightly smaller resolution (in the nm range, depending also on the sample properties!)

The close vicinity between tip and surface realized in AFM opens the way for probing physical **quantities other** than the van der Waals interaction force

For instance, tribological and material quantities can be measured (e.g., friction, viscoelasticity, Young modulus, etc.)
With suitable tips (conductive, magnetic), static and quasi-static electromagnetic forces locally occurring at the sample surface can be analyzed

Lateral Force Microscopy (LFM, SFFM)

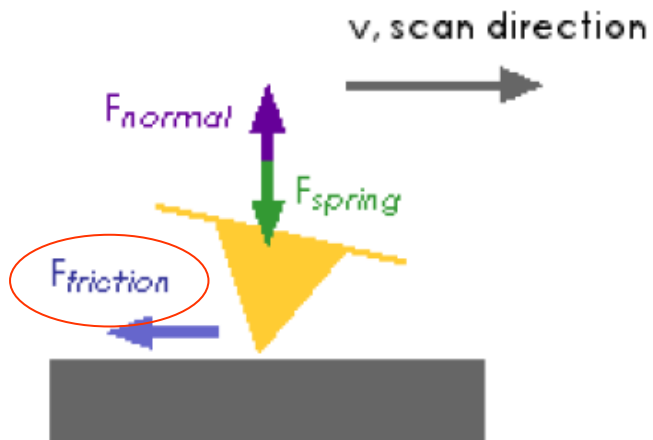


During the scan, the tip is continuously displaced with respect to the surface

Friction forces occur, resulting in a *twisting* of the cantilever

Cantilever twist can be recorded by a two-dimension position sensitive detector (i.e., a 4-quadrant photodetector)

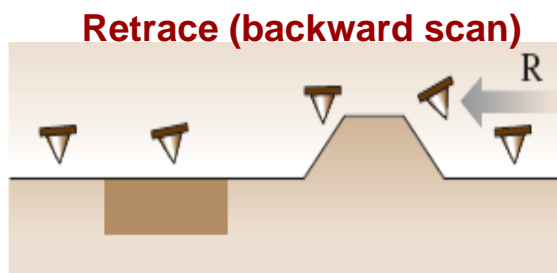
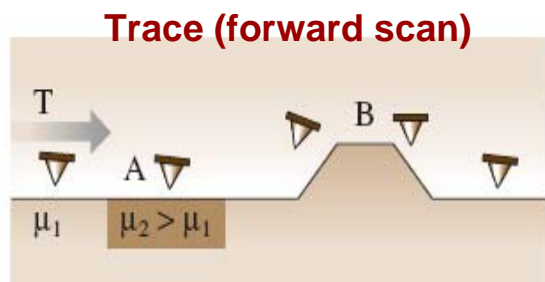
Friction effects can be corrected by the topographical artifacts by comparing forward and backward scans



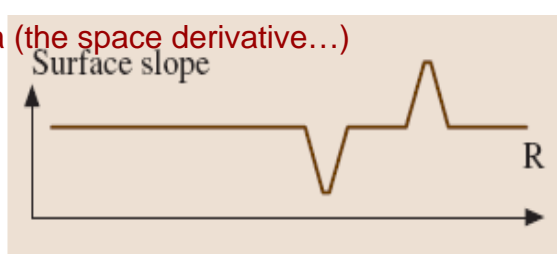
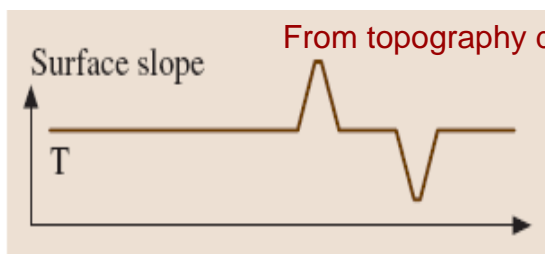
- $(A+B)-(C+D) = \text{normal force (AFM signal)}$
- $(A+C)-(B+D) = \text{lateral force (LFM signal)}$

Materiale tratto dal seminario di Cinzia Rotella, 2006

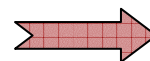
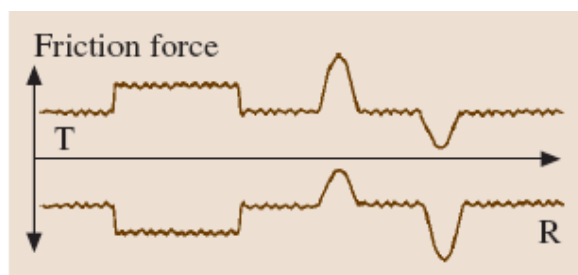
Friction and topography: artifacts and genuine



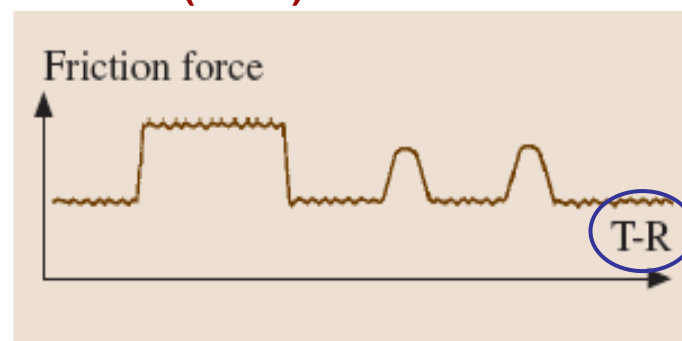
Friction force is **always** oriented against motion!



Lateral force data



(Local) friction data



Lateral force data are always convoluted with topography (slope), but genuine information of the local friction can be derived by comparing trace and retrace and considering simultaneously acquired topography data

Examples of LFM/SFFM images

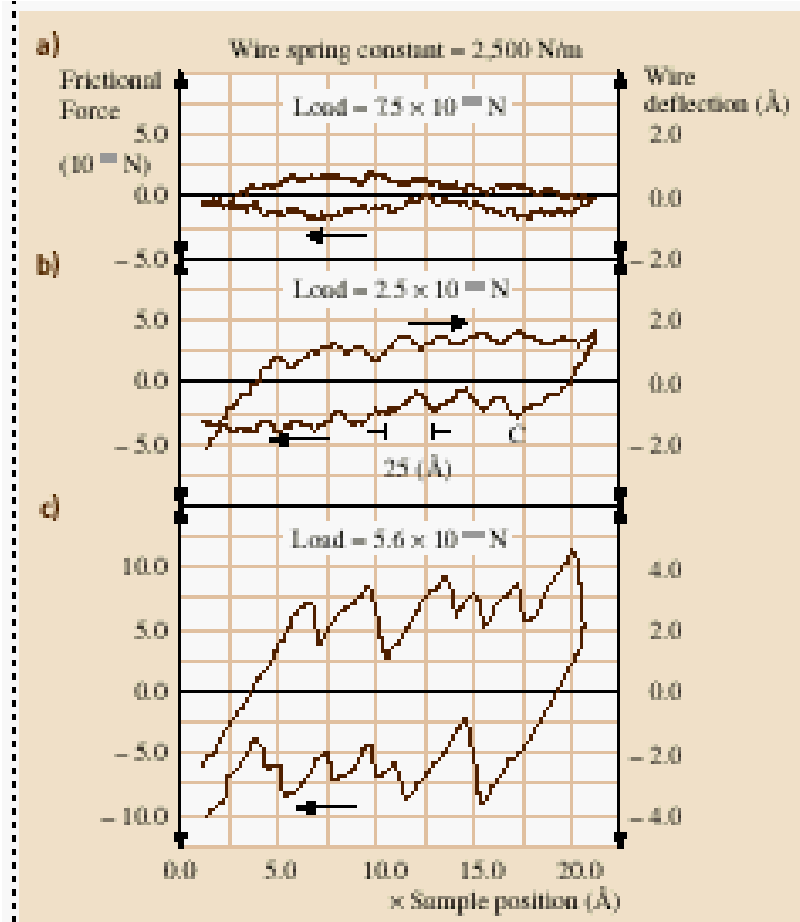


Fig. 20.15a-c Friction loops on graphite acquired with (a) $F_N = 7.5 \mu\text{N}$, (b) $24 \mu\text{N}$ and (c) $75 \mu\text{N}$. (After [20.1])

- ✓ LFM/SFFM offers an additional contrast mechanism
- ✓ Possibility to discriminate different materials at the atom level
- ✓ Nanotribology investigations can be carried out

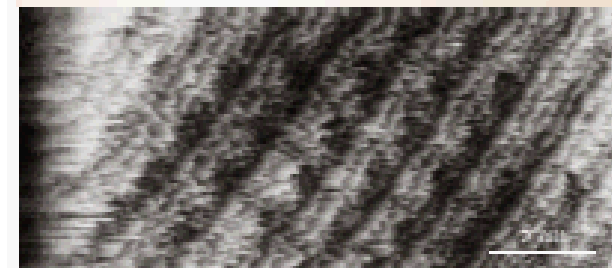


Fig. 20.19 (a) Topography and (b) friction image of Si(111)7x7 measured with a PTFE coated Si-tip. (After [20.29])

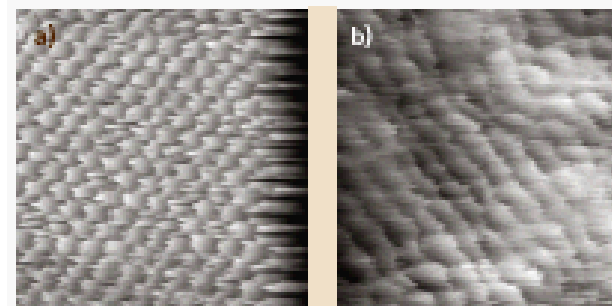
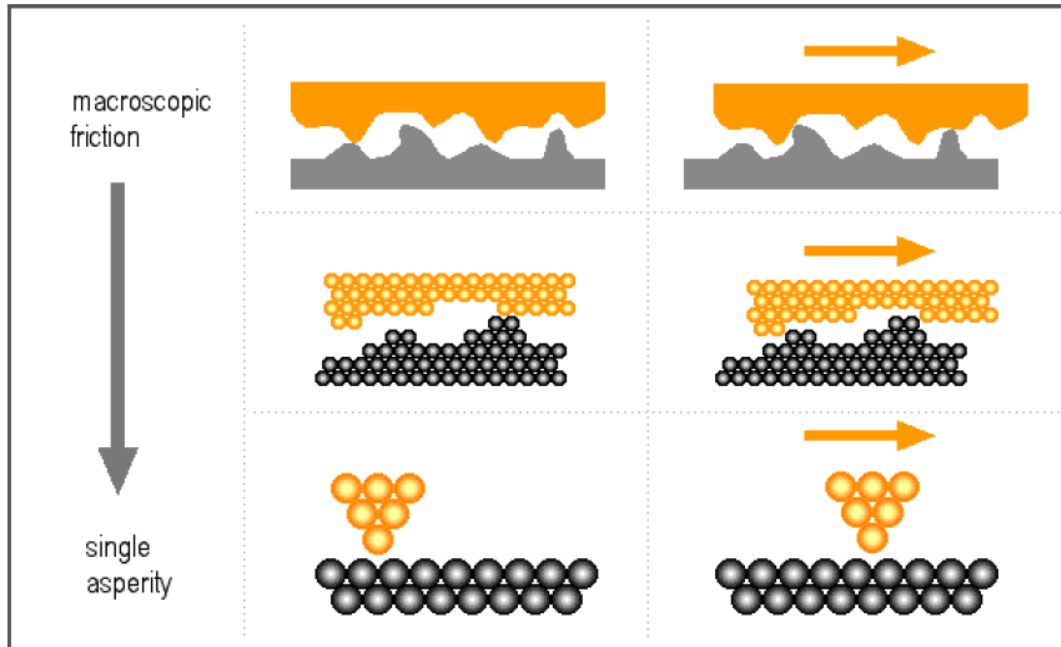


Fig. 20.19a,b Friction images of (a) Ca(111) and (b) Ca(100). Frame size: 3 nm. (After [20.34])

Da B. Bhushan, Handbook of nanotechnology (Springer, 2003)

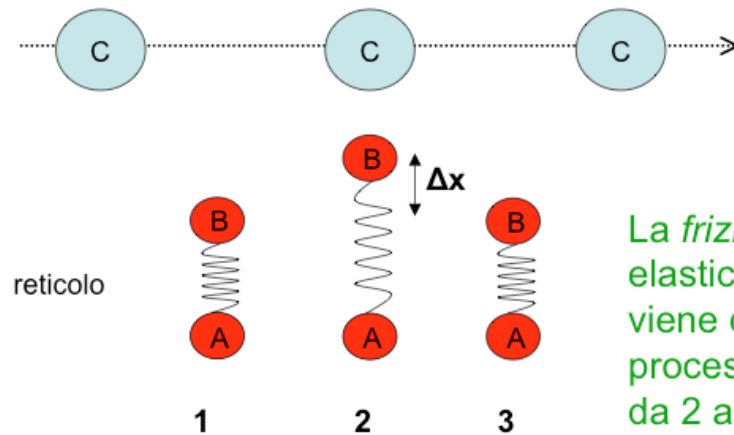
A few words on nanotribology



Sliding motion of the AFM tip “in contact” with the surface turns out affected by “tribological mechanisms” at the atomic scale:

- Adhesion;
- Ploughing;
- Deformation

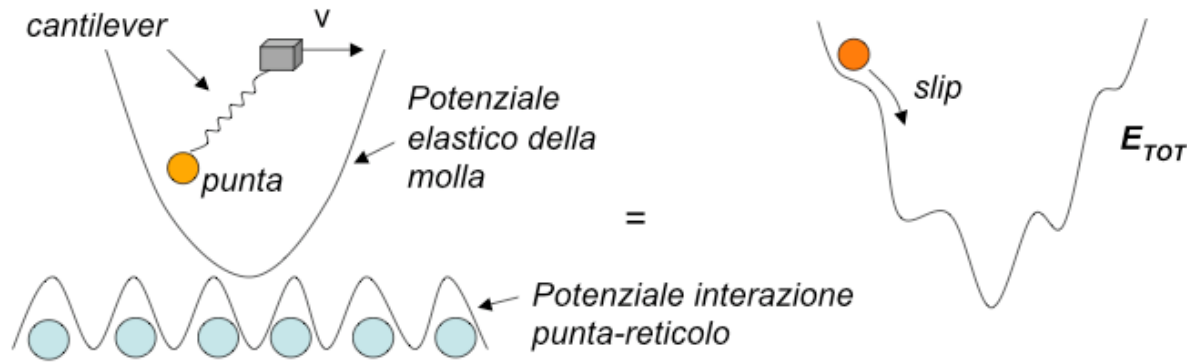
- Modello di Tomlinson (1929) :
modello di attrito applicabile su scala atomica



La *frizione* è l'energia elastica $\frac{1}{2} K(\Delta x)^2$ che viene dissipata nel processo di rilassamento da 2 a 3

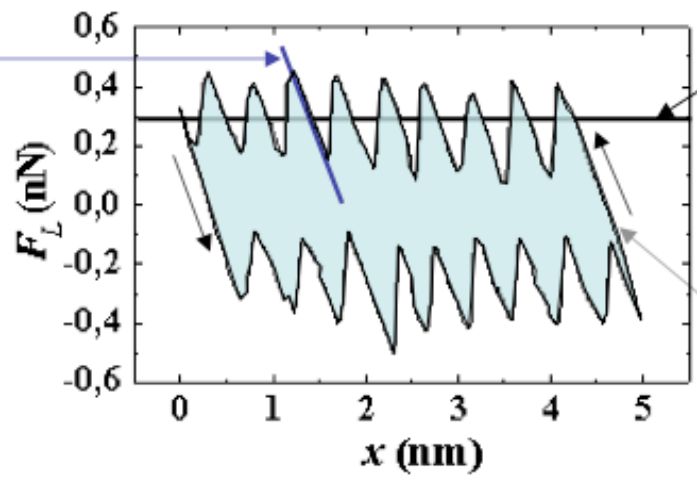
Friction models at the atomic scale must account for local tip /surface interaction

Stick-slip mechanism during the scan



Interaction potential accounts for the periodic surface potential

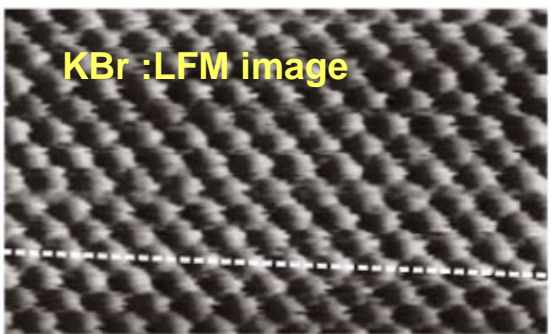
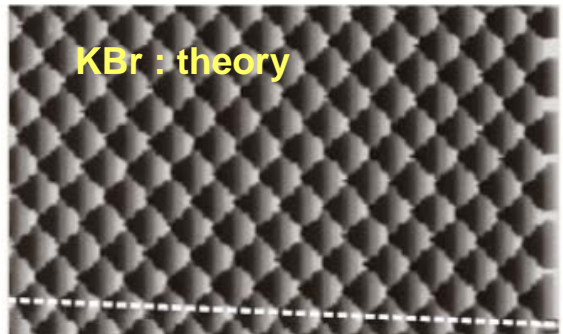
Pendenza nella regione di equilibrio:
costante elastica che rappresenta le interazioni punta-campione
 $1/K_{eff} = 1/K_T + 1/K_C$



Forza laterale media:
permette il calcolo di μ

Area dentro il ciclo di isteresi: energia totale dissipata

Singola linea di scansione LFM di NaCl a $v = 2.5$ nm/s



Detailed and quantitative info can be achieved at the atomic level

Magnetic Force Microscopy (MFM)

3.3.2 Magnetic Scanning Force Microscopy (MFM)

If a magnetic tip is used in the scanning force microscope, magnetic structures can be imaged. Magnetic scanning force microscopy is of interest, in particular, for the investigation of magnetic storage media. In the most general case, the magnetic force between sample and tip is

$$F_{\text{mag}} = -\nabla \int_{\text{tip}} \mathbf{M}_{\text{tip}} \cdot \mathbf{H}_{\text{sample}} dV \quad (13)$$

or

$$F_{\text{mag}} = (\mathbf{m}_{\text{tip}} \nabla) \mathbf{B}_{\text{sample}} \quad (14)$$

where $\mathbf{H}_{\text{sample}}$ and $\mathbf{B}_{\text{sample}}$ are the magnetic stray field and the magnetic induction of the sample, respectively. \mathbf{M}_{tip} and \mathbf{m}_{tip} are the magnetisation and the magnetic moment of the tip, respectively. Since in most cases the exact magnetic structure of the tip is not known, a model tip magnetization must be assumed. In the simplest case, the tip is a spherically structured magnetic single domain with the magnetisation \mathbf{M}_{tip} . Of particular interest are the stray fields of magnetic storage media which consist of different domains. Since the important aspect in force microscopy is not the forces but the force gradient, a pronounced variation of the signal is found near the domain walls, but not inside a domain. This situation is sketched in Figure 21. The parameter of the two curves shown (solid and broken lines) is the ratio of the working distance d and the radius R of the magnetic domain of the tip.

Figure 22a shows an experimentally measured picture of four different oriented magnetic domains. Images b and c show the fine structure of a 180° domain. Alternating bright and dark contrasts can be seen. These contrast changes show that the domain wall consists of segments with different wall orientation. This example illustrates that magnetic SFM is well suited for imaging magnetic structures that are commonly used in today's storage media.

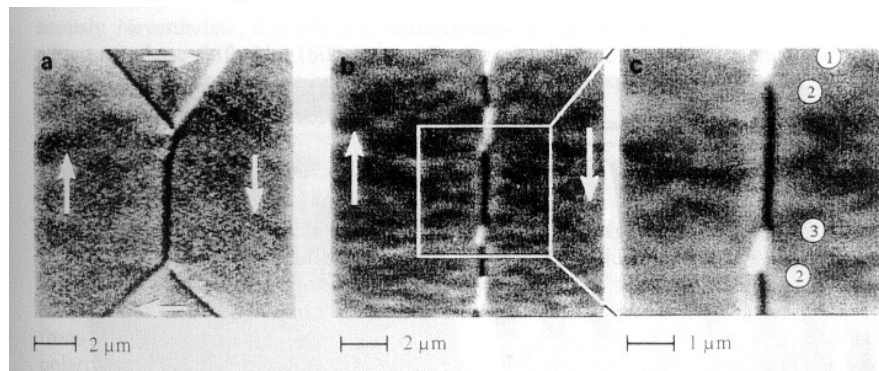


Figure 22: Magnetic SFM image of magnetic domains. (a) shows four domains of a Landau-Lifshitz structure in which the domain walls are the dark and bright lines. (b) and (c) show the fine structure of a 180° domain wall. The domain wall consists of segments with different wall orientation. Arrows denote the domain orientation. (after [26]).

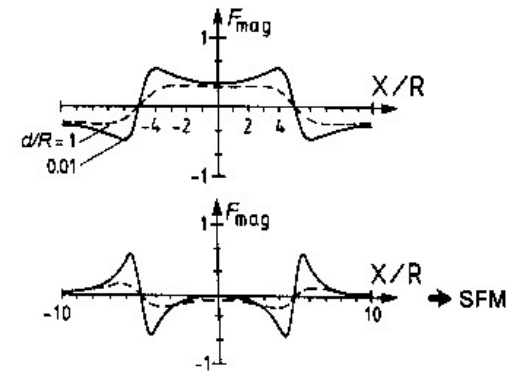
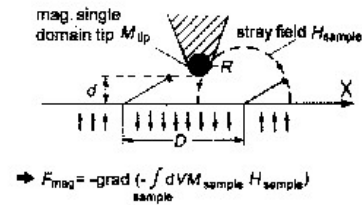


Figure 21: Principle of magnetic scanning force microscopy. On the left, the tip-sample configuration is shown and on the right the force and nominal force constant as a function of distance for this configuration. Two domain walls exist at position 5 (after [23]).

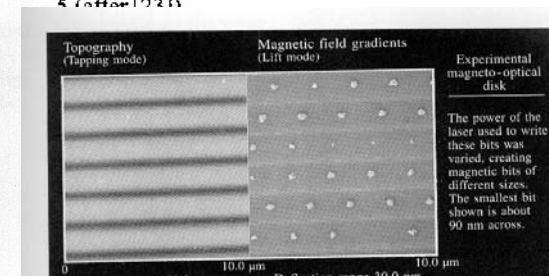


Fig. 5.21. A pair of images of a magneto-optical disk [5.36]

Electrostatic Force Microscopy (EFM)

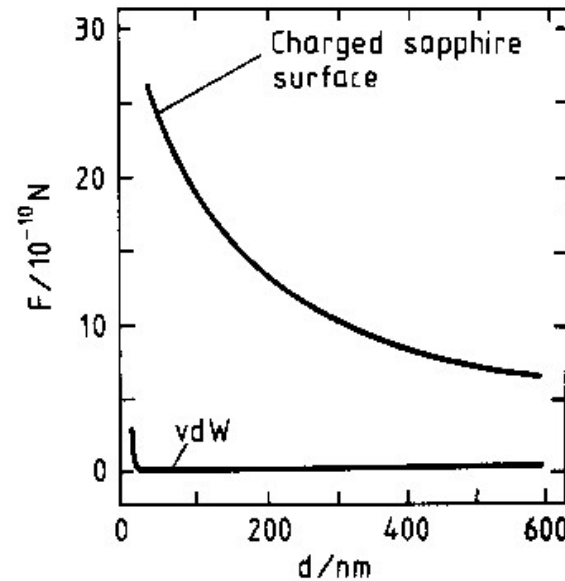
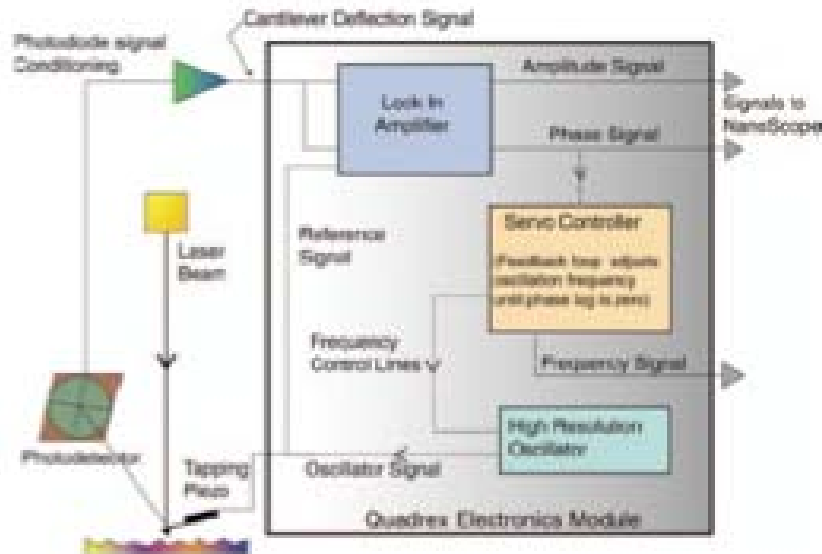


Figure 26: Comparison of the distance dependence of the electrical and van der Waals forces between a tip and a local electrical surface charge of $2 \cdot 10^{-16} \text{ C}$ (after [23]).

Basic idea: application of a ddp between tip at sample in order to be sensitive to electric forces, thus to the space distribution of charges on the sample surface and to its electrostatic potential

Modulation/demodulation techniques used to get direct information on various surface/tip interaction features

Excellent sensitivity to local charges

Application to electronic devices (also in operating conditions)

Application to ferroelectric materials (also known as Piezoelectric Force Microscopy - PFM)

Operating modes in EFM

- Un EFM viene utilizzato principalmente per misurare il potenziale elettrostatico locale della superficie. A tale scopo alla punta viene applicata esternamente una tensione con una componente continua V_{dc} e una componente V_{ac} modulata alla frequenza Ω . Il campione è invece collegato a massa. La forza elettrostatica tra punta e campione è data da [1]:

$$F = \frac{1}{2} \frac{dC}{dz} V^2$$

C rappresenta l'accoppiamento capacitivo tra punta e campione mentre z è la variabile che indica la quota della punta. In V compaiono la tensione applicata ($V_{dc} + V_{ac} \sin \Omega t$) una eventuale tensione indotta sulla punta da altri effetti secondari (V_{ind}) e la tensione locale del campione (V_{cp}).

$$V = (V_{cp} + V_{dc} + V_{ind}) + V_{ac} \sin(\Omega t)$$

La forza elettrostatica tra il campione e la punta può essere scomposta in tre componenti a frequenze diverse:

$$F = \frac{1}{2} \frac{dC}{dz} V^2 = \frac{1}{2} \frac{dC}{dz} [(V_{cp} + V_{dc} + V_{ind}) + V_{ac} \sin(\Omega t)]^2 = F_{dc} + F_{\Omega} + F_{2\Omega}$$

Esaminiamo ora in dettaglio le tre componenti.

- Il primo termine della forza è costante nel tempo ed è pari a:

$$F_{dc} = \frac{1}{2} \frac{dC}{dz} [(V_{cp} + V_{dc} + V_{ind})^2 + \frac{1}{2} V_{ac}^2]$$

- Il secondo termine invece dipende direttamente dalle quantità di interesse come dC/dz o $(V_{cp} + V_{ind})$ ed è modulato alla frequenza Ω :

$$F_{\Omega} = \frac{dC}{dz} (V_{cp} + V_{dc} + V_{ind}) V_{ac} \sin(\Omega t)$$

- Il terzo termine è modulato alla frequenza 2Ω ed è molto importante perché dipende esclusivamente da V_{ac} , che è noto, e da dC/dz :

$$F_{2\Omega} = -\frac{1}{4} \frac{dC}{dz} V_{ac}^2 \cos(2\Omega t)$$

Materiale tratto dal seminario di Nicola Paradiso, 2006

Operazione in modalità nano-Kelvin

Come si è detto precedentemente operando con un EFM occorre fornire una tensione con una componente continua e una modulata. Se con un circuito di reazione noi iniettiamo una tensione V_{dc} tale che il termine $F_{dc} = 0$, per cui $V_{dc} = -(V_{cp} + V_{ind})$, allora potremo misurare variazioni di tensione sulla superficie dovute a sia a V_{cp} che a V_{ind} .

Impiego di un EFM per misure in dc

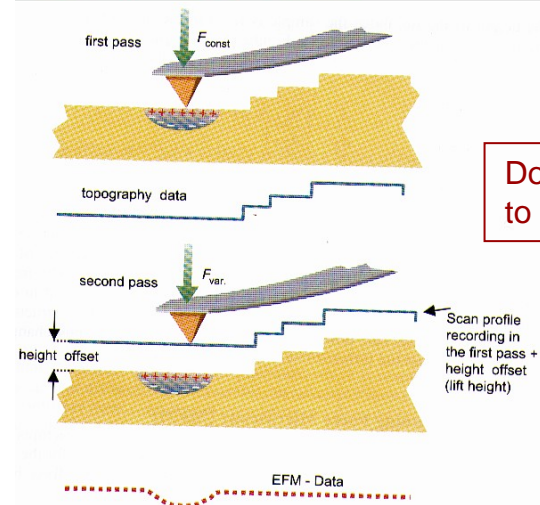
L'utilizzo dell'EFM è basato sull'assunto che la forza elettrostatica sia un effetto al secondo ordine sull'oscillazione meccanica [1]. Tali effetti vengono separati per mezzo di due amplificatori lock-in che permettono di estrarre il segnale modulato alla frequenza Ω e quello alla frequenza 2Ω . E' conveniente scegliere la frequenza Ω in modo da lavorare lontani dalla risonanza di oscillazione meccanica. Come si è detto, conviene inserire anche un circuito di reazione per poter misurare e mappare il potenziale elettrico superficiale. Queste operazioni richiedono che la distanza punta-campione sia stabile durante la misura. Esaminiamo brevemente due metodi che permettono di lavorare in tali condizioni.

Modalità single-pass

Operando in aria, l'ampiezza dell'oscillazione meccanica della cantilever vicina alla risonanza è in genere debolmente dipendente da eventuali interazioni elettrostatiche. Se però localmente i valori di V_{cp} e di V_{ind} diventano molto intensi l'immagine topografica che si ricava può risultare disturbata. In modalità single-pass si utilizzano tensioni dc basse e si acquisiscono simultaneamente i dati sulla topografia (ottenuti facendo oscillare la sonda in tapping mode), i dati del segnale alla frequenza Ω e alla frequenza 2Ω . Operando in modalità nano-Kelvin in pratica si sottrae la tensione V_{cp} che disturba l'immagine, mentre con il segnale alla frequenza 2Ω si ricava il valore dell'accoppiamento capacitivo locale.

Modalità double-pass

Questa modalità prevede un primo passaggio volto ad acquisire il profilo topografico locale. La cantilever viene posta in oscillazione (tapping mode) senza che venga applicata alcuna tensione esterna. Alla fine della scansione della linea, il piezo si ritrae, allontana la sonda dal campione di una certa quantità fissata e riprende la scansione nel senso opposto, mantenendo fissa la quota basandosi sui dati topografici appena acquisiti. In questa fase la punta è relativamente più sensibile alle forze elettrostatiche in quanto forze a lungo range. Nello specifico qui viene rilevata la variazione di fase dovuta al gradiente di forza elettrostatica. Rispetto alla modalità single-pass questa modalità ha il vantaggio di essere più sensibile alle proprietà elettrostatiche del sistema. Lo svantaggio è rappresentato dalla perdita di risoluzione dovuta all'aver aumentato la quota di lavoro.



Examples of EFM images

Electronic devices

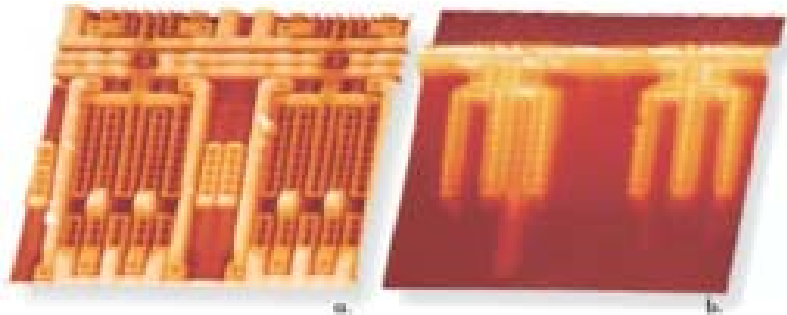


Figure 6. Topography (a) and EFM image (b) of a live packaged IC with passivation layer on. EFM image detects transistor in saturation. 80µm scans.

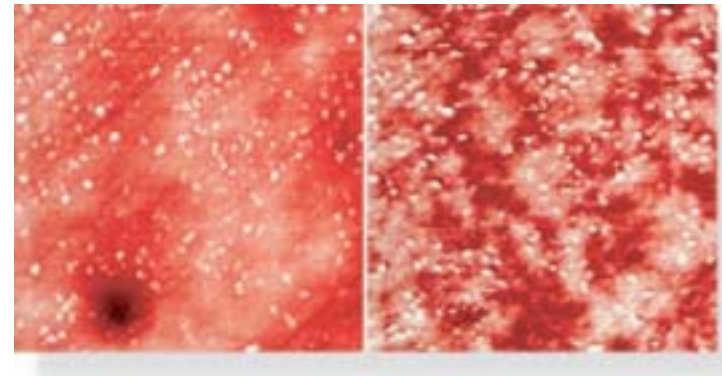
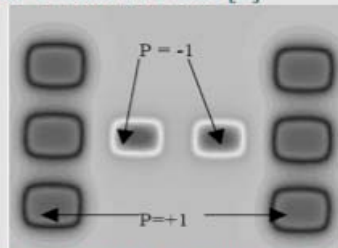


Figure 11. Topography (left) and phase detection EFM (right) images of the surface of a thick-film resistor (TFR). EFM image depicts the conductive RuO₂ network (dark) exposed at the surface. 56µm scans.

Ferroelectric materials

Riportiamo a titolo di esempio l'immagine ricavata dalla scansione di un campione sulla cui superficie sono stati distribuiti dei domini ferroelectrici. L'area esaminata misura 2µm x 3µm, mentre i singoli domini misurano 500nm x 300nm [3].

Domini ferroelectrici depositati su un substrato isolante. E' indicata la polarizzazione normalizzata del campo in corrispondenza dei domini. La distanza tip-sample è stata di 60nm. L'area di scansione misura 2µm x 3µm.



Per materiali che non hanno una polarizzazione permanente vale l'analisi svolta precedentemente. La polarizzazione va calcolata auto-consistentemente; la risoluzione in ogni caso decresce con l'aumentare della separazione tip-sample, come messo in evidenza dalla seguente figura:

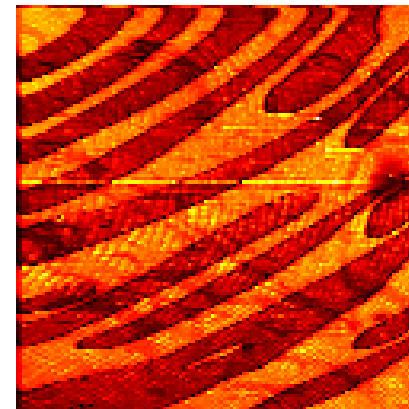


Image of ferroelectric domain structure in TGS Sample by Voltage Modulation Atomic Force Microscopy
Scan size 27 µm x 27 µm

Conclusions

- ✓ Scanning Probe techniques have been developed thanks to advances in material fabrication (atomic probes), electronics (and piezoelectric translators), and *methods of operation* (e.g., the role of feedback)
- ✓ Space resolution is excellent in SPMs (at the “atomic level” for some of them)
- ✓ Most important: physical quantities can be *measured* (in quantitative terms) with SPM, as topographical height, surface density of states, optical properties, ...
- ✓ STM is a powerful method to access local electronic properties of a surface (and, through a suitable feedback system, topography at the atomic level)
- ✓ AFM extends STM capabilities to *any kind* of material surfaces (not restricted to conductive as in STM)
- ✓ AFM “relatives” open the way to a wide variety of local measurements and imaging methods